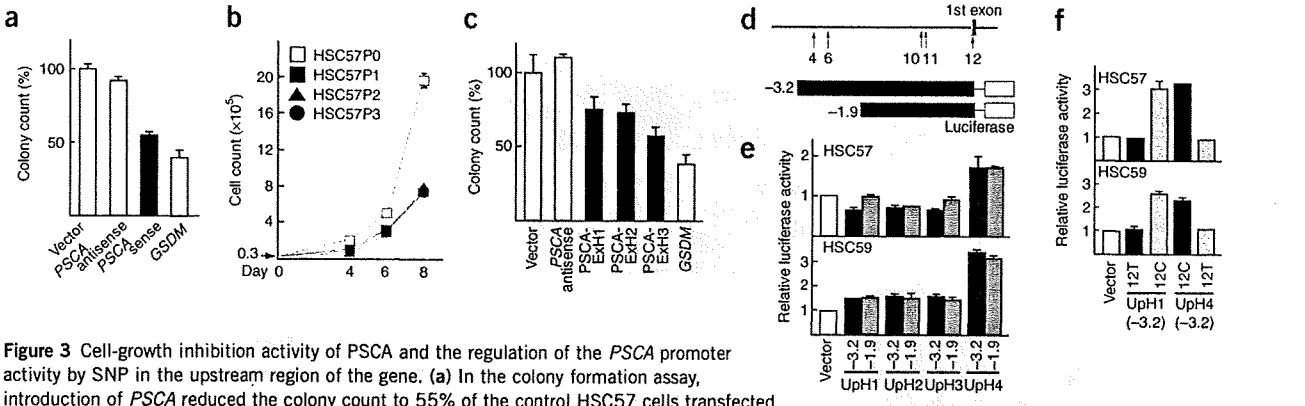

Figure 3 Cell-growth inhibition activity of PSCA and the regulation of the *PSCA* promoter activity by SNP in the upstream region of the gene. **(a)** In the colony formation assay, introduction of *PSCA* reduced the colony count to 55% of the control HSC57 cells transfected with a negative control empty vector. The *GSDM* expression vector was used as a positive control for its cell-proliferation inhibition activity[49]. Error bars, s.d. **(b)** Cell growth assay revealed that the three clones of HSC57 cells, HSC57P1, HSC57P2 and HSC57P3, stably transfected with *PSCA* cDNA showed slower growth rate than the parental HSC57P0, which does not express *PSCA*. **(c)** Colony formation assay showing no significant difference in the cell proliferation inhibition activity among the *PSCA* expression vectors representing the three major haplotypes, ExH1, ExH2 and ExH3, defined by the exonic SNPs (**Table 3**). Repeated experiments are shown in **Supplementary Figure 9** online. **(d)** The 3.2-kb and 1.9-kb upstream fragments cloned in luciferase reporter vectors were prepared by base-substitution to represent each haplotype (UpH1-UpH4) described in **Table 3**. **(e)** Reporter assay revealed a difference in the promoter activity among the 4 haplotypes of the *PSCA* upstream region. **(f)** Substitution of C allele of SNP No.12 (rs2294008) in the PSCA-UpH4(-3.2) for T allele reduced the reporter activity (UpH4(-3.2)-12T), and substitution of T allele of this SNP in the PSCA-UpH1(-3.2) for C increased the reporter activity (UpH1(-3.2)-12C).

The above experiments used *PSCA* cDNA corresponding to the exonic SNP–based haplotype ExH2 (**Table 3**). We next extended the colony formation assay to other haplotypes in order to evaluate their functional differences. *PSCA* cDNA expression constructs were made to represent each of the three major haplotypes covering the exonic regions of the gene (**Table 3** and **Fig. 1b**) by base substitution, and these were introduced to the HSC57 cells. Repeated experiments showed no detectable difference in the suppressive effect on colony formation (**Fig. 3c** and **Supplementary Fig. 9** online). PSCA has an N-terminal signal sequence corresponding to the first 20 residues[20]. *PSCA*-ExH3 has a C allele at rs2294008, which changes the presumed initiation ATG codon to ACG and which may result in a 9-amino-acid truncation of the signal peptide. An *in vitro* translation showed that the product of each haplotype has almost the same size, which is compatible with a difference of only 9 amino acids among the haplotypes (**Supplementary Fig. 10** online). However, a study using EYFP-fusion proteins detected no difference in the subcellular distribution between PSCA-ExH1-EYFP and PSCA-ExH3-EYFP.

Upstream SNP-based haplotypes affect *PSCA* expression

Haplotype analysis deduced four upstream SNP-based haplotypes (**Table 3**), with UpH1 giving the highest odds ratio and UpH4 the least in a one-to-the-others contingency table. To assess the functional significance of the upstream SNPs, we isolated a 3.2-kb genomic fragment including the upstream region and 5′ portion of the first exon of *PSCA*, corresponding to nucleotide positions –3,236 to +28 in relation to the transcription starting site and covering the region from SNPs rs2978981 to rs2294008. Four reporter plasmids constructed by base substitution represent the four haplotypes, designated as PSCA-UpH1(–3.2), PSCA-UpH2(–3.2), PSCA-UpH3(–3.2) and PSCA-UpH4(–3.2) (**Table 3** and **Fig. 3d**). A reporter assay using the HSC59 cells demonstrated that PSCA-UpH4(–3.2) showed the highest luciferase activity, which was 2.5-fold of the activity of the others, and this highest activity was also demonstrated in the assay using the HSC57 cells (**Fig. 3e**). When the C allele of rs2294008 SNP in PSCA-UpH4(–3.2) was replaced by T, the risk allele, the reporter assay showed a reduction of the reporter activity (**Fig. 3f**). In contrast, replacement of the alleles of rs2978981, rs2976387, or rs13262164 by the risk allele did not change the reporter activity (data not shown). The same transcription modulating effect of the haplotypes was also observed for the shorter 1.9-kb version of the *PSCA* upstream region (**Fig. 3e**). The results of the expression and functional analyses suggest that PSCA has an inhibitory effect on cell proliferation and that the rs2294008 SNP can modulate *PSCA* promoter activity.

Replication in Korea

Finally, the association of rs2294008 and rs2976392 was examined at the National Cancer Center (NCC) in Korea on 457 diffuse-type and 418 intestinal-type gastric cancers. Healthy volunteers who visited NCC in Korea for cancer screening provided 390 controls. The two SNPs are also strongly associated in Korea with diffuse-type gastric cancer, but less significantly with intestinal-type cancer (**Table 5**).

DISCUSSION

Through this two-stage genome-wide association study, we identified the *PSCA* gene as a previously unknown susceptibility gene for diffuse-type gastric cancer in Japan. Of the two main categories, the odds ratio was lower and the *P* value higher for the intestinal type, suggesting that *PSCA* is specifically involved in diffuse-type gastric adenocarcinomas. This association pattern was replicated in diffuse- and intestinal-type gastric cancer cases and controls in Korea (**Table 5**). It is notable that the risk alleles exist as major alleles in Japan, whereas the same alleles represent minor alleles in the other HapMap ethnic groups ($P = 5.6 \times 10^{-4}$ and 7.3×10^{-8} against CEU and HCB, respectively, for rs2294008). In Korea, the risk alleles matched those in Japan, but they are also minor alleles in the Korean population (**Supplementary Fig. 11** online).

The odds ratio of *PSCA* SNP rs2294008 in a dominant model was 4.18 (95% CI: 2.88–6.21; **Table 4**), possibly larger than the odds ratio of the –160C/A SNP (rs16260) of *CDH1* (refs. 29–31), the gene implicated in familial and sporadic diffuse-type gastric cancer. Because the –160C/A SNP was not included in the first-stage screening

Table 5 Association of SNPs in *PSCA* with two major gastric cancer types in Korea

	Case genotype			Allele model			Dominant model			Recessive model		
Type	AA	Aa	aa	OR	95% CI	*P* (Fisher)	OR	95% CI	*P* (logistic)	OR	95% CI	*P* (logistic)
rs2976392 (SNP No.19): risk allele (A) frequency in 390 control subjects = 0.463												
Diffuse 449 cases	159	240	50	1.90	1.56–2.33	8.0×10^{-11}	3.47	2.32–5.27	1.1×10^{-10}	1.64	1.17–2.30	0.0036
Intestinal 416 cases	119	213	84	1.37	1.12–1.68	0.0017	1.86	1.27–2.72	0.0010	1.24	0.86–1.80	0.26
390 controls	93	175	122	–	–	–	–	–	–	–	–	–
Intestinal vs. diffuse	–	–	–	1.39	1.14–1.69	9.0×10^{-4}	1.75	1.13–2.74	0.010	1.41	1.01–1.97	0.041
rs2294008 (SNP No. 12): risk allele (T) frequency in 390 control subjects = 0.462												
Diffuse 454 cases	159	246	49	1.91	1.57–2.33	6.3×10^{-11}	3.61	2.41–5.51	3.2×10^{-11}	1.61	1.15–2.26	0.0051
Intestinal 417 cases	118	215	84	1.37	1.12–1.68	0.0017	1.85	1.27–2.71	0.0011	1.22	0.84–1.77	0.31
390 controls	92	176	122	–	–	–	–	–	–	–	–	–
Intestinal vs. diffuse	–	–	–	1.39	1.14–1.69	7.9×10^{-4}	1.81	1.17–2.83	0.0066	1.39	1.00–1.94	0.050

Genotypes are shown as AA for risk allele homozygotes, Aa for heterozygotes and aa for the nonrisk allele homozygotes. For dominant and recessive models, gender- and age-adjusted OR, its 95% CI and *P* values calculated by exact logistic regression are shown. Allele and genotype frequency differences between the intestinal- and diffuse-type gastric cancers were tested for statistical significance.

markers in our genome scan, we genotyped it on 744 diffuse-type gastric cancer cases analyzed in the second-stage genome scan and on 1,397 controls described in **Table 4**. The −160C/A SNP showed a marginally significant protective effect in our diffuse-type gastric cancer cases only in a dominant model ($P = 0.038$, OR = 0.81, 95% CI = 0.66–0.99; **Supplementary Table 2** online).

Although certain transitions and overlaps exist for the two main pathological classifications of gastric cancer, as described earlier, we could still detect a difference between intestinal- and diffuse-type gastric adenocarcinomas with respect to genetic susceptibility. This result is congruous to the proposed notion that two distinct pathways of gastric carcinogenesis exist[32]: one arising in the atrophic gastritis with or without intestinal metaplasia, which develops to the intestinal-type cancer at least initially, and the other arising *de novo* from the gastric epithelial precursor cells, typically leading to diffuse-type cancer. Moreover, our immunohistochemical analysis localized the primary site of the PSCA protein expression at the isthmus of the gastric gland, which is considered to harbor proliferating precursor cells, the presumed origin of diffuse-type gastric adenocarcinoma[2,4]. Thus, the expression pattern may be compatible with the idea that *PSCA* is involved in the susceptibility to diffuse-type gastric cancer.

In this study, information about *H. pylori* infection status was unavailable for most of the subjects, although it is a significant risk factor for both intestinal and diffuse types in Japan, which has a high prevalence of *H. pylori* infection[33]. We do not, however, consider this a major flaw of this study. First, our explanatory variable is an SNP, which is not influenced by *H. pylori* infection. Thus, *H. pylori* infection cannot be a classical confounder, although it could be an intermediate variable between SNP and disease, the former of which may exert its risk effect by modulating the susceptibility of an individual to *H. pylori* infection. In that case, however, we would not want to adjust for *H. pylori* infection, in order not to miss such SNPs in our genome scan. The only important information possibly missed as a result of the lack of *H. pylori* infection data would be the interaction term between it and the SNP. In fact, numerous publications have examined interleukin gene polymorphisms that may increase cancer risk through modulating host response to virulent *H. pylori* strains[34]. However, in Japan, assessing a possible *H. pylori–PSCA* interaction would be difficult, as 99% of Japanese individuals with gastric cancer and 90% of the Japanese adult population are seropositive for *H. pylori*[33].

PSCA encodes a 123-amino-acid glycoprotein with 30% similarity to stem cell antigen 2 (Sca-2), a cell surface marker of immature thymic lymphocytes, and it belongs to the LY-6 family, which shares a glycosylphosphatidylinositol (GPI) anchor domain[20]. Although the function of PSCA is yet to be elucidated, it could have a role in signal transduction, as it is a GPI-anchored membrane protein, and several reports suggest its involvement in cell growth regulation in various systems[27,28,35,36]. *In vitro*, growth of HSC57 cells stably expressing *PSCA* was slower than HSC57 cells expressing no *PSCA* (**Fig. 3b**). Although *PSCA* was overexpressed in prostate cancer cells, it was suppressed in the cancers of the bladder, esophagus, skin and stomach (refs. 22 and 37 and this study). Those findings suggest that *PSCA* is actually expressed in epithelial cells of several tissues other than the prostate and downregulated by malignant transformation, suggesting that PSCA has a tumor suppressor–like character in certain types of cancers, although its roles in prostate cancer may differ.

Because the rs2294008 SNP may alter the first methionine, a polymorphic variation is possible in the length of the N-terminal signal peptide, which in turn can lead to a difference in protein folding, intracellular processing or subcellular localization. However, our *in vitro* analyses including the colony formation assays could detect no difference among the major haplotypes of the *PSCA* exonic regions. On the other hand, a reporter assay showed that rs2294008 can modulate transcriptional activity of the upstream region of *PSCA*. Because of strong LD between rs2294008 and rs2976392 ($r^2 = 0.995$, $D' = 0.999$), the *PSCA* gene was first identified by association with the latter SNP; however, we propose that the functional SNP is the former, rs2294008. Although the actual effect of the SNP *in vivo* is unknown and we could not exclude its possible effect on function of the N-terminal signal sequence, the risk allele, T, is associated with lower transcriptional activity of the supposedly tumor-suppressive *PSCA* gene, at least in the context of the −1.9 kb and −3.2 kb upstream regions of the gene.

Validating the allele-dependent difference in the transcriptional activity *in vivo* proved difficult in our preliminary experiments. We examined a small sample set of noncancerous stomach portions surgically dissected for gastric cancer. However, a quantitative RT-PCR analysis demonstrated no clear relationship between *PSCA* expression and the haplotypes (data not shown). Laser microdissection is at least necessary, but we may still need to normalize the value

of *PSCA* expression by the value of another reference gene whose expression is unique to *PSCA*-expressing cells. Such a reference gene is not yet established.

Finally, **Table 1** shows another candidate genomic region on chromosome 1 for association with diffuse-type gastric cancer that is statistically significant by permutation test and even by Bonferroni correction for multiple testing. The region contains multiple genes in the extended LD block and awaits future investigation. Once most of the common but low-penetrance polymorphisms are identified for this disease, the typing of these variants would have significant diagnostic power to promote a personalized preventive medicine[38]. Until such a collection is established, this line of research may contribute mostly to the understanding of carcinogenesis mechanisms.

METHODS

Classification of gastric adenocarcinoma and case selection. In Japan, pathological diagnosis of gastric cancer includes both macroscopic and microscopic (histological) typing of the gastric resection specimen according to the Japanese classification system of gastric carcinoma[39]. Histologically, the common type of gastric cancer is classified into seven categories: papillary adenocarcinoma (pap), tubular adenocarcinoma (tub1 and tub2), poorly differentiated adenocarcinoma (por1 and por2), signet-ring cell carcinoma (sig) and mucinous adenocarcinoma (muc). However, Lauren's classification of gastric cancer into two major categories, intestinal and diffuse types[3], is also widely used, especially for research purposes. In Korea, the pathohistological classification is based on Lauren's system and WHO classification[40]. The relationship of the three classification systems is shown in **Supplementary Table 1** online. In addition to these histological types, the Japanese system identifies types 0 to 5 by macroscopic examination: type 0 corresponds to early gastric cancer in most of the cases and is further subdivided into five subtypes, including a superficial depressed subtype, type 0 IIc. Linitis plastica, a highly malignant diffusely infiltrating form of gastric carcinoma, is type 4, which is almost always the diffuse type by histological classification[8,40].

The original purpose of this study was to identify genetic predisposition to linitis plastica, and we hypothesized that its typical precursor lesions should look like those of type 0 IIc. Therefore, we set linitis plastica as the case selection criterion for the stage 1 screening of the genome scan in Japan. For the stage 2 screening, we expanded inclusion criteria to include type 0 IIc with por2 or sig type histology. For the analysis of intestinal-type gastric cancers, we included pap, tub1 and tub2 by histological diagnosis and excluded type 4 by macroscopic examination.

In the replication study in Korea, the inclusion criterion for diffuse-type gastric cancer was linitis plastica or Lauren's diffuse type with poorly differentiated or signet-ring cell type histology by WHO classification. The inclusion criterion for intestinal-type gastric cancer was Lauren's intestinal type with papillary or well-differentiated or moderately differentiated type histology in WHO classification, and the exclusion criterion was linitis plastica.

Study design and subjects. In the first-stage screening of the genome scan, each SNP was genotyped on 188 cases and 752 controls. Because some DNA samples were used up and had to be replaced with other samples in the middle of the SNP-by-SNP typing in this genome scan, a total of 194 DNA samples (107 males and 87 females, mean age of 57 years) were obtained from individuals with the linitis plastica type of gastric cancer. The germline DNA was extracted either from peripheral blood leukocytes, from methanol-fixed paraffin-embedded tissues of noncancerous gastric mucosa or lymph nodes[41], or from fresh noncancerous gastric mucosa dissected by operation. The control or reference samples of the first screening were a combined group of the individuals with four other diseases in the joint five-disease genome scan project (Millennium Genome Project in Japan)[18]; the reference genotype frequency data were obtained on 752 subjects (188 individuals for each of the four diseases) per SNP from the total of 190 individuals with Alzheimer's disease, 213 with type 2 diabetes, 189 with hypertension, and 194 with asthma. The reference DNA samples were extracted from peripheral blood leukocytes.

In the following second-stage screening and a subsequent high-density SNP typing of the *PSCA* gene, 763 DNA samples from individuals with gastric cancer (male 403, mean age 56; female 360, mean age 55) were extracted either from methanol-fixed paraffin-embedded tissues of noncancerous gastric mucosa or lymph nodes or from peripheral blood of individuals with the linitis plastica type of gastric cancer (165 cases) or early-stage cancer diagnosed as macroscopic type 0 IIc with histological type of por2 and/or sig[39] (598 cases). The gastric cancer samples were collected at six institutions as follows: 365 paraffin-embedded tissues and 167 blood samples by the National Cancer Center Hospital in Tokyo, 128 blood samples by Nippon Medical School Hospital in Tokyo, 57 blood samples by Aichi Cancer Center in Aichi, 23 blood samples by Shikoku Cancer Center in Ehime, 19 blood samples by Hiroshima University Graduate School of Biomedical Sciences in Hiroshima and 4 blood samples by Hamamatsu University School of Medicine in Shizuoka. The control DNA samples for the second screening and for the high-density SNP typing on *PSCA* were from peripheral blood leukocytes of 751 volunteer individuals (male 387, mean age 55; female 364, mean age 54) with no known malignancies who offered blood at the occasion of a health check examination at two institutions: 204 and 335 individuals at Keio University campuses in Kanagawa and Tokyo, respectively, and 212 at Iwata City Hospital in Shizuoka. As in the first-stage screening, samples for 14 gastric cancer cases and a control were exhausted and replaced with another 15 samples; the final valid typing data were obtained on 749 cases and 750 controls for the second screening and also for the high-density typing of *PSCA*.

To construct an LD map around the *PSCA* gene, we obtained genotype data from a control population of 379 Japanese volunteers from the Iwata City Hospital (108 males), National Cancer Center (60 females) and Keio University (211 females).

Resequencing of *PSCA* was also done on DNA samples from 48 healthy Japanese volunteers at Keio University campuses, 47 of whom were not included in the control subjects genotyped in the second screening of the genome scan.

We obtained genotype data on the 11 *PSCA* SNPs for 599 intestinal-type gastric cancer cases and 648 controls. The DNA samples were extracted from 433 methanol-fixed paraffin-embedded tissue archives of noncancerous gastric mucosa or lymph nodes in the National Cancer Center Hospital and from 166 peripheral blood leukocytes from individuals at Nippon Medical School Hospital. The 648 control samples were derived from peripheral blood leukocytes of volunteers at Iwata City Hospital, who were different individuals from the 212 control Iwata subjects genotyped in the second screening by Invader assay. Therefore, data on the 11 *PSCA* SNPs were available for a total of 1,399 (751 + 648) control subjects.

In the Korean study, peripheral blood samples were donated from individuals with gastric cancer who were diagnosed or treated in the National Cancer Center in Seoul, Korea. The control subjects were volunteers who participated in the National Cancer Screening Program at the National Cancer Center and who were confirmed not to have gastric cancer by an endoscopy. The sample size of at least 350 subjects in each group was designed to provide the study with 90% power to detect an association of a SNP with minor allele frequency of 0.38 and allelic odds ratio of 1.45 in a two-sided test at a significance level of 5%.

Age and gender distributions of the subjects are shown in **Supplementary Figure 12** online. The Japanese part of the study was approved by the ethics committees of the participating institutions in accordance with the Ethics Guidelines For Human Genome/Gene Analysis Research in Japan. The Korean component of the gastric cancer case-control study was approved by the ethics committee of the National Cancer Center, Korea. Informed consent was obtained from all living subjects, including opt-out consent for the paraffin-block archival samples.

Depending on the samples, some restrictions may apply for sharing human materials with readers because of limited availability or conditions of the original informed consent.

Genotyping and resequencing. Genotyping for stages 1 and 2 of the genome scan was done using the Invader (Third Wave Technologies) assay combined with multiplex PCR[42], with some modifications such as the use of only 10 ng of genomic DNA in 10 μl total reaction volume. Fine typing of the *PSCA* region

was done on the SNPs selected by the resequencing data using either the Invader or TaqMan SNP Genotyping (Applied Biosystems) assays. We genotyped the intestinal-type gastric cancer cases and controls using Illumina GoldenGate assay (Illumina) developed for 14 SNPs of *PSCA*, with success on 11 SNPs. Part of genotype data to calculate linkage disequilibrium of the *PSCA*-containing genomic region was obtained by Sentrix Human-1 Genotyping BeadChip (Illumina). All the Korean samples were genotyped in the National Cancer Center, Korea by TaqMan SNP Genotyping Assays.

The Invader assay is a SNP-by-SNP genotyping system, and we excluded SNP markers that showed significant deviation from the Hardy-Weinberg equilibrium (χ^2 P value <0.001) in any of the reference disease groups. A final genotype call was made by visual quality-check inspection of SNP cluster plots of normalized fluorescence intensities. In the stage 1 screening, we genotyped 100,000 SNPs identified by the JSNP project and obtained 85,925 SNPs that passed our strict quality control process. After removing some SNPs that did not have JSNP ID assignment at that time, we subjected 85,576 SNPs to statistical analysis. In the stage 2 screening, 2,880 SNPs were genotyped, and 2,753 passed quality control.

Resequencing of *PSCA* was done on 48 control individuals using BigDye Terminator v1.1 Cycle Sequencing Kit and ABI PRISM 3700 DNA Analyzer (Applied Biosystems). The sequencing covered nucleotide positions 143,755,899 to 143,761,136 (NCBI Build 36), except for about 300 bp of sequence (for example, 143,757,522–143,757,748, 143,759,074–143,759,094, 143,760,414–143,760,439 and 143,760,801–143,760,837), because of difficulties in primer design.

Statistical analyses. The statistical power of this two-stage genome-wide scan study has been described elsewhere[18,23]. The statistical significance of the association was evaluated for each SNP by Fisher's exact tests. Crude odds ratios for allele, dominant and recessive inheritance models were calculated in the first-stage screening, in which two sets of control or reference data were used: one was the allele and genotype frequency data of the combined group of individuals with four other diseases (see above), and the other was the allele frequency reference data of the general Japanese population (752 individuals) available from the JSNP database (JSNP reference data). The SNPs subjected to the second stage of the genome scan were selected by the following step-wise procedure: (i) the SNPs were excluded if their minor allele frequencies were less than 0.1 in the JSNP reference data, (ii) the SNPs were excluded if they were not mapped on autosomal chromosomes, (iii) the odds ratios and P values against the JSNP reference data were ignored if the allele frequencies of the JSNP reference data and those of the reference disease group were significantly different (that is, P value $<10^{-4}$), (iv) the odds ratios and P values for the reference disease group were ignored if the reference disease group consisted of only one disease as a result of quality control of typing data, (v) genotype odds ratios and P values for the reference disease group were ignored when the P value for Hardy-Weinberg equilibrium was less than 0.01 in the reference disease group, (vi) the SNPs were excluded if their genotype odds ratios were less than 1.5 and allelic odds ratios were less than 1.3, (vii) the SNPs were excluded if the risk allele or genotypes against the reference disease group were opposite to those against the JSNP control data, (viii) the top 4,000 SNPs were selected without redundancy in the order of increasing P values by Fisher's exact tests, and (ix) pair-wise LD parameters were estimated among the 4,000 SNPs, and the SNP with a lower P value was selected from each pair of the SNPs showing a high LD parameter (r^2 >0.9). Finally, we selected 2,880 SNPs for the stage 2 typing, which generated valid data on 2,753 SNPs after a quality check process.

The significance of association in the second screening was evaluated at the significance level of 0.05 by multiple testing using Bonferroni correction and permutation test[43]. Assuming 2,753 independent hypothesis tests, the conservative Bonferroni correction requires a P value of 1.8×10^{-5} before correction. Odds ratios adjusted for three age categories ($\leq$39, 40–59 and $\geq$60) and gender were also calculated by exact logistic regression for dominant and recessive models for the stage 2 screening data and in the Korean replication study (**Supplementary Fig. 12**).

The haplotype-based association was tested on the basis of Wald statistics, which were obtained by CHAPLIN[44] case-control haplotype inference software, assuming a multiplicative model. Other statistical analyses were carried out using the Statistical Analysis System software version 9.1 (SAS Institute) and the R suite.

To evaluate the effect of population stratification in this study, we examined the population structure by the STRUCTURE software[45], the Genomic Control[46] and mixture model[47] methods using 1,025 and 501 loci from the stage 1 and 2 samples, respectively. None of the three analyses detected a significant subpopulation in the stage 1 or 2 samples after removing 28 samples from the 26 pairs and 1 trio that showed more than a 65% genotype concordance rate within the total of 980 samples analyzed in the first-stage genotyping. These samples may represent duplication, identical twins or first-degree relatives, depending on the degree of the concordance (**Supplementary Note** online). Even if we revise the first-stage screening data by removing 5 gastric cancer cases and 23 other-disease reference samples from the groups showing the high genotype concordance rate, 9 of the 10 SNPs listed in **Table 1** are nevertheless selected for the stage 2 screening, but the fourth SNP, rs3804775, does not pass the selection criteria because of its low odds ratio.

The genotype frequency data for the first and second screening are available in the GeMDBJ database (see URLs section below). Because the first-screening data may be used as an independent reference dataset by database users, the revised, 'cleaned-up' data after removing the high concordance samples are presented in the public database to minimize a spurious stratification.

Linkage disequilibrium analysis. LD analysis of the *PSCA-LY6K* region was done using genotype data of 379 control individuals obtained by Illumina Human-1 BeadChip, which contains 28 SNPs that reside in and around the *PSCA* gene: rs4587307, rs6988393, rs750529, rs2976399, rs2294008, rs2976391, rs2920298, rs2920297, rs2976394, rs10216533, rs2976395, rs1045547, rs1045605, rs1435453, rs2585174, rs2585153, rs4736323, rs7822193, rs2585187, rs13362, rs2585126, rs2239703, rs2572925, rs3750246, rs3764795, rs3802226, rs3819496 and rs3819497. The pattern of LD was analyzed using two parameters, r^2 and D' (ref. 48).

Functional analyses. Materials and methods for preparation of antibody to PSCA, immunohistochemistry, laser-captured microdissection and RT-PCR, cDNA isolation, colony formation assay, cell growth assay and reporter assay are described in the **Supplementary Methods** and **Supplementary Table 3** online.

URLs. JSNP database, http://snp.ims.u-tokyo.ac.jp/; GeMDBJ database, http://gemdbj.nibio.go.jp/.

Note: Supplementary information is available on the Nature Genetics website.

ACKNOWLEDGMENTS

This work was supported in Japan by the program for promotion of Fundamental Studies in Health Sciences of the National Institute of Biomedical Innovation (NiBio) and by Health and Labour Sciences Research Grants by Ministry of Health, Labour and Welfare. The Korean part of the study was supported by grant 0710340 from the National Cancer Center, Korea.
We thank the following people (listed in alphabetical order) for discussion and technical and statistical assistance: M. Asako, T. Chujo, C. Hamada, T. Hayashida, C. Hirama, F. Igarashi, T. Imai, E. Inoue, S. Kamakami, A. Katoh, O. Kawaguchi, C. Kina, N. Kurata, Y. Liu, G. Maeno, S. Mimaki, N. Mitsuhashi, N. Miyahara, A. Miyaoka, R. Nakajima, J. Nakata, Y. Odaka, T. Ogiwara, N. Ohsawa, E. Ohshima, M. Okada, M. Okuyama, Y. Sakashita, M. Sato, M. Seishi, T. Sobue, H. Suganami, E. Takemoto, T. Taniguchi, S. Uchida, T. Urushidate, M. Ushiama, S. Yabe, N. Yamaguchi, S. Yamamoto and I. Yoshimura.

AUTHOR CONTRIBUTIONS

Principal investigators: H. Sakamoto, K. Yoshimura and N.S. **Gastric cancer project planning and design:** H. Sakamoto, K. Yoshimura, T.Y., H.K. and T.S. **Ascertainment of subjects for genetic analyses:** H.K., T.S., Y.M., D.S., H. Sugimura, F.T., S.K., N. Matsukura, N. Matsuda, T. Nakamura, I. Hyodo, T. Nishina, W.Y., H.H., M.H., E.T. and S.H. **Genetic analyses:** H. Sakamoto, Sumiko Ohnami, A.S. and Y.N. **Statistical analyses and database:** K. Yoshimura, Y.S., H.T., M.A., R.T., Y.T., M.O., K. Aoki, I. Honmyo and S.C. **Functional analyses:** N.S., K. Aoyagi, H. Sasaki, Sumiko Ohnami, Shunpei Ohnami, K. Yanagihara and H. Sakamoto. **National Cancer Center, Korea:** K.-A.Y., M.-C.K., Y.-S.L., S.R.P., C.G.K. and I.J.C. **Millennium Genome Project Cancer Subteam Leader:** T.Y. **Millennium Genome Project Human Genome Variation Team Leader:** Y.N. **Millennium Genome Project Disease Gene Team Leader:** S.H.

Published online at http://www.nature.com/naturegenetics/
Reprints and permissions information is available online at http://npg.nature.com/reprintsandpermissions/

1. Crew, K.D. & Neugut, A.I. Epidemiology of gastric cancer. *World J. Gastroenterol.* **12**, 354–362 (2006).
2. Ushijima, T. & Sasako, M. Focus on gastric cancer. *Cancer Cell* **5**, 121–125 (2004).
3. Lauren, P. The two histological main types of gastric carcinoma: diffuse and so-called intestinal-type carcinoma. An attempt at a histo-clinical classification. *Acta Pathol. Microbiol. Scand.* **64**, 31–49 (1965).
4. Hohenberger, P. & Gretschel, S. Gastric cancer. *Lancet* **362**, 305–315 (2003).
5. Saito, A., Shimoda, T., Nakanishi, Y., Ochiai, A. & Toda, G. Histologic heterogeneity and mucin phenotypic expression in early gastric cancer. *Pathol. Int.* **51**, 165–171 (2001).
6. Machado, J.C. *et al.* E-cadherin gene mutations provide a genetic basis for the phenotypic divergence of mixed gastric carcinomas. *Lab. Invest.* **79**, 459–465 (1999).
7. Schier, S. & Wright, N.A. Stem cell relationships and the origin of gastrointestinal cancer. *Oncology* **69**(Suppl. 1), 9–13 (2005).
8. Rosai, J. in *Rosai and Ackerman's Surgical Pathology*, Ch. 11, Gastrointestinal tract—stomach 648–711 (Mosby, Edinburgh, 2004).
9. Japanese Gastric Cancer Association Registration Committee. Gastric cancer treated in 1991 in Japan: data analysis of nationwide registry. *Gastric Cancer* **9**, 51–66 (2006).
10. Yokota, T. *et al.* Borrmann's type IV gastric cancer: clinicopathologic analysis. *Can. J. Surg.* **42**, 371–376 (1999).
11. Henson, D.E., Dittus, C., Younes, M., Nguyen, H. & Albores-Saavedra, J. Differential trend in the intestinal and diffuse types of gastric carcinoma in United States, 1973–2000 – increase in the signet ring cell type. *Arch. Pathol. Lab. Med.* **128**, 765–770 (2004).
12. Shinmura, K. *et al.* Familial gastric cancer: clinicopathological characteristics, RER phenotype and germline *p53* and *E-cadherin* mutations. *Carcinogenesis* **20**, 1127–1131 (1999).
13. Lichtenstein, P. *et al.* Environmental and heritable factors in the causation of cancer: analyses of cohorts of twins from Sweden, Denmark, and Finland. *N. Engl. J. Med.* **343**, 78–85 (2000).
14. Correa, P. & Shiao, Y.-H. Phenotypic and genotypic events in gastric carcinogenesis. *Cancer Res.* **54** (7 Suppl.), 1941s–1943s (1994).
15. González, C.A., Sala, N. & Capellá, G. Genetic susceptibility and gastric cancer risk. *Int. J. Cancer* **100**, 249–260 (2002).
16. Hirakawa, M. *et al.* JSNP: a database of common gene variations in the Japanese population. *Nucleic Acids Res.* **30**, 158–162 (2002).
17. Haga, H., Yamada, R., Nakamura, Y. & Tanaka, T. Gene-based SNP discovery as part of the Japanese Millennium Genome Project: identification of 190,562 genetic variations in the human genome. *J. Hum. Genet.* **47**, 605–610 (2002).
18. Yoshida, T. & Yoshimura, K. Outline of disease gene hunting approaches in the Millennium Genome Project of Japan. *Proc. Jpn. Acad.* **79**, 34–50 (2003).
19. Kato, N. *et al.* High-density association study and nomination of susceptibility genes for hypertension in the Japanese National Project. *Hum. Mol. Genet.* **17**, 617–627 (2008).
20. Reiter, R.E. *et al.* Prostate stem cell antigen: a cell surface marker overexpressed in prostate cancer. *Proc. Natl. Acad. Sci. USA* **95**, 1735–1740 (1998).
21. Gu, Z. *et al.* Prostate stem cell antigen (PSCA) expression increases with high gleason score, advanced stage and bone metastasis in prostate cancer. *Oncogene* **19**, 1288–1296 (2000).
22. Bahrenberg, G., Brauers, A., Joost, H.-G. & Jakse, G. Reduced expression of *PSCA*, a member of the LY-6 family of cell surface antigen, in bladder, esophagus, and stomach tumors. *Biochem. Biophys. Res. Commun.* **275**, 783–788 (2000).
23. Sato, Y. *et al.* Designing a multistage, SNP-based, genome screen for common diseases. *J. Hum. Genet.* **49**, 669–676 (2004).
24. Karam, S. & Leblond, C.P. Origin and migratory pathways of the eleven epithelial cell types present in the body of the mouse stomach. *Microsc. Res. Tech.* **31**, 193–214 (1995).
25. Karam, S.M., Straiton, T., Hassen, W.M. & Leblond, C.P. Defining epithelial cell progenitors in the human oxyntic mucosa. *Stem Cells* **21**, 322–336 (2003).
26. Fukaya, M. *et al.* Hedgehog signal activation in gastric pit cell and in diffuse-type gastric cancer. *Gastroenterology* **131**, 14–29 (2006).
27. Saffran, D.C. *et al.* Anti-PSCA mAbs inhibit tumor growth and metastasis formation and prolong the survival of mice bearing human prostate cancer xenografts. *Proc. Natl. Acad. Sci. USA* **98**, 2658–2663 (2001).
28. Gu, Z., Yamashiro, J., Kono, E. & Reiter, R.E. Anti-prostate stem cell antigen monoclonal antibody 1G8 induces cell death *in vitro* and inhibits tumor growth *in vivo* via a Fc-independent mechanism. *Cancer Res.* **65**, 9495–9500 (2005).
29. Wang, G.-Y., Lu, C.-Q., Zhang, R.-M., Hu, X.-H. & Luo, Z.W. The E-cadherin gene polymorphism -160C/A and cancer risk: A HuGE review and meta-analysis of 26 case-control studies. *Am. J. Epidemiol.* **167**, 7–14 (2008).
30. Humar, B. *et al.* Association of *CDH1* haplotypes with susceptibility to sporadic diffuse gastric cancer. *Oncogene* **21**, 8192–8195 (2002).
31. Pharoah, P.D. *et al. CDH1* c-160a promotor polymorphism is not associated with risk of stomach cancer. *Int. J. Cancer* **101**, 196–197 (2002).
32. Smith, M.G., Hold, G.L., Tahara, E. & El-Omar, E.M. Cellular and molecular aspects of gastric cancer. *World J. Gastroenterol.* **12**, 2979–2990 (2006).
33. Sasazuki, S. *et al.* Effect of *Helicobacter pylori* infection combined with CagA and pepsinogen status on gastric cancer development among Japanese men and women: a nested case-control study. *Cancer Epidemiol. Biomarkers Prev.* **15**, 1341–1347 (2006).
34. Kamangar, F., Cheng, C., Abnet, C.C. & Rabkin, C.S. Interleukin-1B polymorphisms and gastric cancer risk-a meta-analysis. *Cancer Epidemiol. Biomarkers Prev.* **15**, 1920–1928 (2006).
35. Tran, C.P., Lin, C., Yamashiro, J. & Reiter, R.E. Prostate stem cell antigen is a marker of late intermediate prostate epithelial cells. *Mol. Cancer Res.* **1**, 113–121 (2002).
36. Sharom, F.J. & Radeva, G. GPI-anchored cleavage in the regulation of transmembrane signals. in *Subcellular Biochemistry, Volume 37: Membrane Dynamics and Domains* (ed. Quinn, P.J.) 285–315 (Kluwer Academic/Plenum Publishers, New York, 2004).
37. De Nooij-van Dalen, A.G. *et al.* Characterization of the human LY-6 antigens, the newly annotated member LY-6K included, as molecular markers for head-and-neck squamous cell carcinoma. *Int. J. Cancer* **103**, 768–774 (2003).
38. Pharoah, P.D. *et al.* Polygenic susceptibility to breast cancer and implications for prevention. *Nat. Genet.* **31**, 33–36 (2002).
39. Japanese Gastric Cancer Association. Japanese classification of gastric carcinoma. - 2nd English edition *Gastric Cancer* **1**, 10–24 (1998).
40. Fenoglio-Preiser, C. *et al.* Gastric carcinoma. in *WHO Classification of Tumours: Tumours of the Digestive System* (eds. Hamilton, S.R. & Aaltonen, L.A.) 39–52 (IARC Press, Lyon, 2000).
41. Noguchi, M., Furuya, S., Takeuchi, T. & Hirohashi, S. Modified formalin and methanol fixation methods for molecular biological and morphological analyses. *Pathol. Int.* **47**, 685–691 (1997).
42. Ohnishi, Y. *et al.* A high-throughput SNP typing system for genome-wide association studies. *J. Hum. Genet.* **46**, 471–477 (2001).
43. Hirschhorn, J.N. & Daly, M.J. Genome-wide association studies for common diseases and complex traits. *Nat. Rev. Genet.* **6**, 95–108 (2005).
44. Epstein, M.P. & Satten, G.A. Inference on haplotype effects in case-control studies using unphased genotype data. *Am. J. Hum. Genet.* **73**, 1316–1329 (2003).
45. Falush, D., Stephens, M. & Pritchard, J.K. Inference of population structure using multilocus genotype data: linked loci and correlated allele frequencies. *Genetics* **164**, 1567–1587 (2003).
46. Bacanu, S.-A., Devlin, B. & Roeder, K. The power of genomic control. *Am. J. Hum. Genet.* **66**, 1933–1944 (2000).
47. Zhu, X., Zhang, S., Zhao, H. & Cooper, R.S. Association mapping, using a mixture model for complex traits. *Genet. Epidemiol.* **23**, 181–196 (2002).
48. Nei, M. *Molecular Evolutionary Genetics* (Columbia University Press, New York, 1987).
49. Saeki, N. *et al. GASDERMIN*, suppressed frequently in gastric cancer, is a target of LMO1 in TGF-beta-dependent apoptotic signalling. *Oncogene* **26**, 6488–6498 (2007).

The full list of authors is as follows:

Hiromi Sakamoto[1,24], Kimio Yoshimura[1,2,24], Norihisa Saeki[1,24], Hitoshi Katai[3], Tadakazu Shimoda[4], Yoshihiro Matsuno[4], Daizo Saito[3], Haruhiko Sugimura[5], Fumihiko Tanioka[6], Shunji Kato[7], Norio Matsukura[7], Noriko Matsuda[7], Tsuneya Nakamura[8], Ichinosuke Hyodo[9,23], Tomohiro Nishina[9], Wataru Yasui[10], Hiroshi Hirose[11], Matsuhiko Hayashi[11], Emi Toshiro[3], Sumiko Ohnami[1], Akihiro Sekine[12], Yasunori Sato[1], Hirohiko Totsuka[13], Masataka Ando[14], Ryo Takemura[15], Yoriko Takahashi[16], Minoru Ohdaira[16], Kenichi Aoki[16], Izumi Honmyo[16], Suenori Chiku[17], Kazuhiko Aoyagi[1], Hiroki Sasaki[1], Shumpei Ohnami[18], Kazuyoshi Yanagihara[19], Kyong-Ah Yoon[20], Myeong-Cherl Kook[20], Yeon-Su Lee[20], Sook Ryun Park[20], Chan Gyoo Kim[20], Il Ju Choi[20], Teruhiko Yoshida[1], Yusuke Nakamura[12,21] & Setsuo Hirohashi[22]

[1]Genetics Division, National Cancer Center Research Institute, 5-1-1 Tsukiji, Chuo-ku, Tokyo 104-0045, Japan. [2]Department of Health Policy and Management, Keio University School of Medicine, 35 Shinanomachi, Shinjuku-ku, Tokyo 160-8582, Japan. [3]Department of Surgical Oncology and [4]Pathology of Clinical Laboratory Division, National Cancer Center Hospital, 5-1-1 Tsukiji, Chuo-ku, Tokyo 104-0045, Japan. [5]First Department of Pathology, Hamamatsu University School of Medicine, 1-20-1 Handayama, Hamamatsu-shi, Shizuoka 431-3192, Japan. [6]Iwata City Hospital, 512-3 Ohkubo, Iwata-shi, Shizuoka 438-8550, Japan. [7]Department of Surgery, Nippon Medical School Hospital, 1-1-5 Sendagi, Bunkyo-ku, Tokyo 113-8602, Japan. [8]Department of Endoscopy, Aichi Cancer Center Hospital, 1-1 Kanokoden, Chikusa-ku, Nagoya 464-8681, Japan. [9]Department of Internal Medicine, Shikoku Cancer Center, 160 Kou, Minamiumemoto-cho, Matsuyama-shi, Ehime 791-0280, Japan. [10]Department of Molecular Pathology, Hiroshima University Graduate School of Biomedical Sciences, 1-2-3 Kasumi, Minami-ku, Hiroshima 734-8551, Japan. [11]Department of Internal Medicine, Keio University School of Medicine, 35 Shinanomachi, Shinjuku-ku, Tokyo 160-8582, Japan. [12]SNP Research Center, The Institute of Physical and Chemical Research (RIKEN), 1-7-22 Suehiro-cho, Tsurumi-ku, Yokohama, Kanagawa, 230-0045, Japan. [13]Bioinfomatics Group, Research and Development Center, Solution Division 4, Hitachi Government and Public Corporation System Engineering Ltd., 2-4-18 Toyo, Koto-ku, Tokyo 135-8633, Japan. [14]Bio-IT Business Promotion Center, Solution Development Laboratories, NEC Corporation, NEC, 5-7-1 Shiba, Minato-ku, Tokyo 108-8001, Japan. [15]Statistical Genetics Analysis Division, StaGen Co., Ltd., Kuramae Orashion Bldg. 9F, 4-31-10 Kuramae Taito-ku, Tokyo 111-0051, Japan. [16]Mitsui Knowledge Industry Co., Ltd., Hitotsubashi SI bldg., 3-26 Kandanishiki-cho, Chiyoda-ku, Tokyo 101-0054, Japan. [17]Science Solutions Division, Mizuho Information and Research Institute, Inc., 2-3 Kanda-nishiki-cho, Chiyoda-ku, Tokyo 101-8443, Japan. [18]Central RI Laboratory and [19]Central Animal Laboratory, National Cancer Center Research Institute, 5-1-1 Tsukiji, Chuo-ku, Tokyo 104-0045, Japan. [20]Research Institute and Hospital, National Cancer Center, 809 Madu 1-dong, Ilsandong-gu, Goyang-si, Gyeonggi-do, 411-764, Korea. [21]Human Genome Center, Institute of Medical Science, University of Tokyo, 4-6-1 Shirokanedai, Minato-ku, Tokyo 108-8639, Japan. [22]National Cancer Center, 5-1-1 Tsukiji, Chuo-ku, Tokyo 104-0045, Japan. [23]Present address: Division of Gastroenterology, Graduate School of Comprehensive Human Sciences, University of Tsukuba, 1-1-1 Tennoudai, Tsukuba, Ibaraki 305-8575, Japan. [24]These authors contributed equally to this work. Correspondence should be addressed to T.Y. (tyoshida@ncc.go.jp).

High mobility group box-1-inducible melanoma inhibitory activity is associated with nodal metastasis and lymphangiogenesis in oral squamous cell carcinoma

Tomonori Sasahira,[1] Tadaaki Kirita,[2] Naohide Oue,[3] Ujjal Kumar Bhawal,[1] Kazuhiko Yamamoto,[2] Kiyomu Fujii,[1] Hitoshi Ohmori,[1] Yi Luo,[1] Wataru Yasui,[3] Anja Katrin Bosserhoff[4] and Hiroki Kuniyasu[1,5]

[1]Department of Molecular Pathology, and [2]Department of Oral and Maxillofacial Surgery, Nara Medical University School of Medicine, Kashihara; [3]Department of Molecular Pathology, Hiroshima University Graduates School of Biochemical Sciences, Hiroshima, Japan; [4]Institute of Pathology, University of Regensburg, Regensburg, Germany

(Received February 5, 2008/Revised May 12, 2008; May 26 2008/Accepted May 26, 2008/Online publication July 4, 2008)

Melanoma inhibitory activity (MIA) is an 11-kDa secretory protein isolated from malignant melanoma cells that is correlated with invasion and metastasis in various human malignancies. We examined MIA expression in 62 oral squamous cell carcinomas (OSCC) by immunohistochemistry. MIA expression was significantly associated with nodal metastasis ($P = 0.00018$). MIA expression was also associated with expression of high mobility group box-1 (HMGB1) ($P < 0.0001$) and lymph vessel density ($P < 0.0001$). Expression levels of MIA, HMGB1, nuclear factor kB (NFkB) p65 and HMGB1–NFkB p65 binding were significantly higher in a metastatic human OSCC cell line (HSC3) than those in a non-metastatic OSCC cell line (HSC4). Treatment with receptor for advanced glycation end products (RAGE) antisense or small interfering RNA and human recombinant HMGB1 (hrHMGB1) did not affect MIA expression, whereas HMGB1 antisense or siRNA treatment decreased MIA expression in HSC3 cells. Then HMGB1 enhanced MIA expression as an NFkB cofactor but not as a RAGE ligand. MIA neutralization by MIA antibodies increased extracellular signal-related kinase 1/2 phosphorylation, but decreased p38 phosphorylation and the expression of vascular epithelial growth factor (VEGF)-C and -D. Treatment with p38 inihibitor decreased VEGF-C and -D expression in HSC3 cells. These results suggest that MIA expression is enhanced by the interaction of intracellular HMGB1 and NFkBp65 and MIA is closely involved in tumor progression and nodal metastasis by the increments of VEGF-C and VEGF-D in OSCC. (*Cancer Sci* 2008; 99: 1806–1812)

Head and neck cancer is the sixth most common malignancy worldwide and the first leading cause of cancer death in South Asia.[1] About 300 000 patients develop OSCC every year in the world.[2,3] OSCC has a high potential for nodal metastasis and locoregional invasion,[4] from which over 50% of patients die.[5,6] To control lymph-node metastasis of OSCC, we need to study the molecular aspects of the mechanism of metastasis.

MIA is an 11-kDa secretory protein isolated from supernatants of HTZ-19 malignant melanoma cells,[7,8] the gene locus of which is mapped to chromosome 19q13.32–13.33.[9] Although previous reports indicated that MIA is correlated with invasion and metastasis in malignant melanoma,[10–12] breast cancer,[10] chondrosarcoma,[13] glioma,[14] and pancreatic cancer,[15] the definite functions of MIA for cancer cells are still unclear.

HMGB1 has a dual role as an extracellular secretory protein and a chromosomal structural protein.[16] HMGB1 works as a cytokine or a growth factor in neural ontogenesis, septic inflammation and neoplasm. HMGB1 is also considered an amphoterin, which is isolated as a motility factor in neurite outgrowth.[17] We previously reported coexpression of HMGB1 and receptor for advanced glycation end products (RAGE), which is a major membrane receptor for HMGB1 and is significantly associated with tumor progression and metastasis[18–24] and suppression of tumor-associated macrophages.[25,26] As a chromatin structural protein, HMGB1 participates in gene expression, DNA repair and functions of the p53 family.[27] Recently, HMGB1 was revealed to interact with NFkB p65 to accelerate MIA expression.[28,29] HMGB1 and NFkB p65 concurrently bind to a 30-bp region in the promoter region of the MIA gene designated as the highly conserved region (HCR).

MIA is suspected to play an important role as a pro-metastatic factor in HMGB1-overexpressing cancers. In the present study, we analyzed the relationship between MIA expression and nodal metastasis and HMGB1 expression in human OSCC.

Materials and Methods

Tumor specimens. Sixty-two formalin-fixed, paraffin-embedded specimens of primary OSCC were randomly selected at Nara Medical University Hospital, Kashihara, Japan. None of the samples was treated using neo-adjuvant therapy. Medical records and prognostic follow-up data were obtained from the patient database administered by the hospital. None of the patients was treated before surgery and sample preparation.

Immunohistochemistry. Consecutive 4-μm sections were cut from each block. Immunohistochemistry was performed as previously described.[24] The sections were subjected to antigen retrieval with pepsin (DAKO, Carpinteria, CA, USA) treatment for 20 min and the immunoperoxidase technique was used in immunostaining. After blockade of endogeneous peroxidase activity by incubation in 3% hydrogen peroxide–methanol for 15 min, the sections were rinsed with phosphate-buffered saline (PBS) and incubated with diluted primary antibodies: Anti-MIA antibody,[10] anti-HMGB1 antibody (Upstate biotechnology, Lake Placid, NY, USA; diluted to 0.5%) and anti-D2-40 antibody (a marker for lymph duct endothelial cells recognizing sialo-glycoprotein type O, Signet Laboratories Inc., Dedham, MA, USA; diluted to 0.5%). After 2 h incubation at room temperature, they were rinsed again with PBS and treated for an hour with the secondary antibody peroxidase-conjugated antigoat (Medical & Biological Laboratories, Nagoya, Japan) or antirabbit

[5]To whom correspondence should be addressed. E-mail: cooninh@zb4.so-net.ne.jp
Abbreviation: OSCC, oral squamous cell carcinoma; MIA, melanoma inhibitory activity; HMGB1, high mobility group box-1; RAGE, receptor for advanced glycation end products; NFkB, nuclear factor kB.

doi: 10.1111/j.1349-7006.2008.00894.x

(Medical & Biological Laboratories) diluted to 0.5%. All sections were then rinsed with PBS, color-developed using diaminobenzidine (DAB) solution (DAKO), washed in water and counterstained with Meyer's hematoxylin (Sigma Chemical, St. Louis, MO, USA). Immunostaining of all samples was performed under the same conditions of antibody reaction and DAB exposure.

Evaluation of immunoreactivity. Immunoreactivity was classified according to Allred's score (AS).[30] We divided the immunoreactivity into four grades by AS: Grade 0, AS is 0; Grade 1, AS is 2–4; Grade 2, AS is 5–6; Grade 3, AS is 7–8. MIA positiveness was exhibited as grades 2 and 3. Labeling index for HMGB1 was calculated as follows: (the number of the HMGB1 positive nucleus/total number of the nucleus) × 100. Anti-D2-40 immunostained specimens were observed under 200× magnification microscopy and three maximum lymph vessel density (LVD) fields were selected from around of the tumor cells (the 'hot spot'). These fields were captured by digital imaging with charge coupled device camera (Olympus, Tokyo, Japan). LVD and mean lymph vessel area (MLA) were measured on the computer-captured image using NIH Image software (National Institutes of Health, Bethesda, MD, USA).

Cell culture. Human OSCC cell lines, HSC3 and HSC4, were studied. HSC3 cells are tongue squamous cell carcinoma-derived metastatic cell lines, which provide many sublines with high metastatic potential. In contrast, HSC4 cells show low metastatic potential. No metastatic sublines are derived from HSC4 cells.[31] Controlled cell line was used for U937 (monocytic leukemia cell line, purchased from Dainihon Pharmaceutical, Tokyo, Japan). All cells were maintained in Roswell Park Memorial Institute medium (RPMI)-1640 (Sigma Chemical) supplemented with 10% fetal bovine serum (Sigma Chemical Co) in 5% CO_2 and 95% air at 37°C. Anti-MIA antibody was used for neutralizing MIA (Santa Cruz Biotechnology) in cultured medium at 2 μL/mL concentration. Rabbit serum (DAKO) was used for control. The cells were also treated with p38 mitogen-activated protein kinase (MAPK) inhibitor SB239063 (Sigma Chemical) at 5 μM for 12 h.

Short interferent RNA. FlexiTube short interferent RNA (siRNA) for MIA, RAGE and HMGB1 were purchased from Qiagen Genomics (Bothell, WA, USA). AllStars Negative Control siRNA was used for control (Qiagen Genomics). These cells were transfected with 50-nM siRNA for each gene using Lipofectamine 2000 (Invitrogen, Carlsbad, CA, USA) according to the manufacturer's instructions.

Antisense phosphorothioate(S)-oligodeoxynucleotide assay. The 18-mer S-oligodeoxynucleotide (ODN) for antisense sequence from 6th to 23rd nucleotide of RAGE cDNA (GenBank AB036432) and the 18-mer S-ODN for antisense sequence from 1st to 18th nucleotide of HMGB1 cDNA (GenBank X12597) were synthesized and purified by reverse-phase high performance liquid chromatography (Sigma Genosys, Ishikari, Japan). The sequence of RAGE antisense was 5′-CTG CTT CCT TCC AGG GTC-3′; the sequence of HMGB1 antisense was 5′-AGG ATC TCC TTT GCC CAT-3′. The sense sequence of the antisense S-ODN was used for the control S-ODN. These cells were pretreated with 3 μM of antisense or sense S-ODN for 6 days with medium exchange and an addition of antisense or sense S-ODN every 2 days. After pretreatment, the cells were used for further experiments. Cytotoxicity of the antisense S-ODN were not relevant at the working concentration.[19]

Immunoblot analysis. Whole-cell lysates were prepared as described previously.[26] Fifty-microgram lysates were subjected to immunoblot analysis in 12.5% sodium dodecyl sulfate–polyacrylamide gels followed by electrotransfer to nitrocellulose filters. The filters were incubated with primary antibody and then with peroxidase-conjugated immunoglobulin G antibody (Medical and Biological Laboratories, Nagoya, Japan). A γ-tubulin antibody was used to assess the levels of protein loaded per lane (Oncogene Research Products, Cambridge, MA, USA). The immune complex was visualized using an enhanced chemiluminescence Western-blot detection system (Amersham, Aylesbury, UK). The primary antibodies used were anti-MIA, anti-NFkB p65, anti-VEGF-C, anti-VEGF-D, anti-ERK1/2, antiphospho-ERK1/2, antiphospho-p38 (Santa Cruz Biotechnology), anti-integrin α5β1 (Serotec Ltd, Oxford, UK) and anti-HMGB1 (Upstate Biotechnology).

Immunoprecipitation. For immunoprecipitation, the lysates were precleaned in a lysis buffer containing protein A/G agarose (Santa Cruz Biotechnology) for 1 h at 4°C and subsequently centrifuged. The supernatants were incubated with anti-HMGB1 antibody (Upstate Biotechnology), or anti NFkB p65 antibody (Santa Cruz Biotechnology) and protein A/G agarose for 3 h at 4°C. The precipitates were collected by centrifugation and washed 5 times with lysis buffer for sodium dodecylsulfate polyacrylamide gel electrophoresis (SDS-PAGE). For loading control, 5 μL of each preimmunoprecipitated sample (lysate diluted with buffer) was slot-blotted onto nitrocellulose membrane and stained with Coomassie blue.

Reverse transcriptase–polymerase chain reaction. Total RNA was extracted from cultured cells using the RNeasy Mini Kit (Qiagen Genomics). Total RNA (1 μg) was converted to cDNA with the First-Strand cDNA Synthesis Kit (Amersham Biosciences, Piscataway, NJ, USA). PCR were performed using Amplitaq Gold Kit (Applied Biosynthesis, Foster City, CA, USA) according to the manufacturer's instructions.

Primer pairs used are listed below: MIA (referred to GenBank NM006533), Sense: 5′-ACCCTA TCT CCA TGG CTG TG-3′, Antisense: 5′-AGG TTT CAG GGT CTG GTC CT-3′; RAGE (referred to GenBank NM172197), Sense: 5′-GCT GTC AGC ATC AGC ATC AT-3′, Antisense: 5′-ATT CAG TTC TGC ACG CTC CT-3′; HMGB1 (referred to GenBank NM002128), Sense: 5′-ATA TGG CAA AAG CGG ACA AG-3′, Antisense: 5′-GCA ACA TCA CCA ATG GAC AG-37; VEGF-C (referred to GenBank NM005429), Sense: 5′-GGA AAG AAG TTC CAC CAC CA-3′, Antisense: 5′-TTT GTT AGC ATG GAC CCA CA-3′; VEGF-D (referred to GenBank NM004469), Sense: 5′-AGG ACT GGA AGC TGT GGA GA-3′, Antisense: 5′-ATC GGA ACA CGT TCA CAC AA-3′; β-actin (referred to GenBank NM001101), Sense: 5′-CAA GAG ATG GCC ACG GCT GCT-3′, Antisense: 5′-TCC TTC TGC ATC CTG TCG GCA-3′. All primers were synthesized by Sigma Genosys (Ishikari, Japan).

Statistical analyses. Statistical differences in MIA expression were tested with the two-tailed χ^2 test. All statistics were calculated using StatView version 4.5 (SAS Institute, Cary, NC, USA) and a *P*-value of less than 0.05 was considered statistically significant.

Results

Relationship between MIA expression and clinical parameters. We examined MIA expression in 62 cases of OSCC (Table 1). Expression of MIA was observed in 48.4% of all cases (30/62). Immunoreactivity for MIA was found in the cell membrane and cytoplasm, except in the nuclei of the cancer cells, but was not found in normal epithelium of all cases (Fig. 1).

A significant association was found between MIA immunoreactivity and histological metastasis of lymph nodes. Four of 23 cases (17.4%) without nodal metastasis (n-) expressed MIA, whereas MIA expression was found in 26 of 39 (66.7%) cases with nodal metastasis (n+) ($P = 0.00018$). Representative cases showed significant MIA expression in the nodal metastatic foci (Fig. 1, MIA in metastasis). HMGB1 labeling indices were also high in the nodal metastatic foci (Fig. 1, HMGB1 in metastasis). However, no significant relationship was found between MIA grading and other parameters: age, sex, primary site, histological differentiation, T classification (extension of primary tumor), clinical stage, tumor recurrence and disease-free survival. To

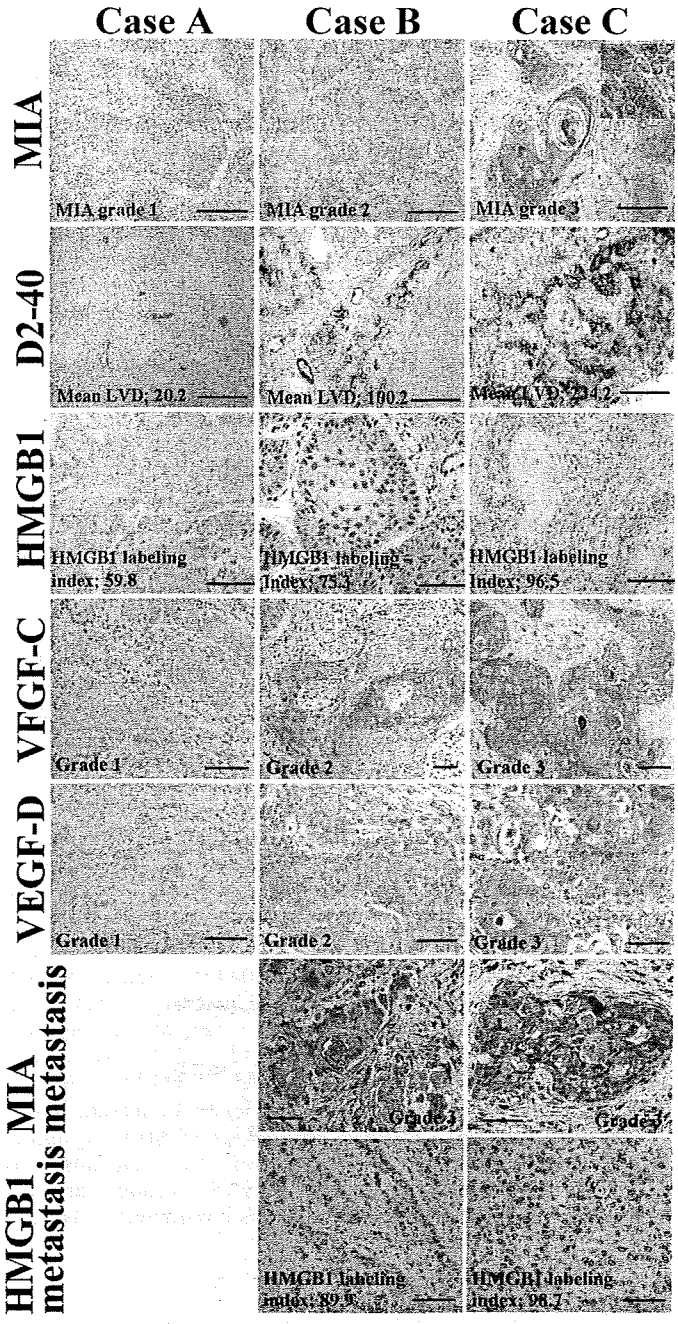

Fig. 1. Immunohistochemical staining of melanoma inhibitory activity (MIA), D2-40, high mobility group box-1 (HMGB1), vascular endothelial growth factor (VEGF)-C and VEGF-D in oral squamous cell carcinomas (OSCC). The expressions of D2-40, HMGB1, VEGF-C and VEGF-D were shown in case A (T2N0M0, stage II, well differentiated OSCC), case B (T2N1M0, stage III, well differentiated OSCC) and case C (T4N2M0, stage IV, well differentiated OSCC). Inset showed MIA localization at the cytoplasm and cytoplasmic membrane. Expressions of MIA and HMGB1 were examined in lymph node metastasis in case B and C. Bar, 100 μm.

confirm significance of MIA to lymph-node metastasis in OSCC, we examined LVD and MLA in tumor tissues (Fig. 2a,b). Lymph vessels around the tumor cells were detected by a lymph duct endothelial marker, D2-40 (Fig. 1). A significant correlation was observed between grading of MIA immunoreactivity and LVD ($P < 0.0001$) or MLA ($P < 0.0001$).

As a chromatin structural protein, HMGB1 is reported to participate in MIA transcription in association with NFkB.[28,29]

Table 1. Relationship between melanoma inhibitory activity (MIA) expression and clinicopathological parameters in oral squamous cell carcinoma (OSCC) patients

	n	MIA expression		*P*-value†
		Negative	Positive	
Age				
–60	43	25	18	
60–	19	7	12	NS
Sex				
Male	35	17	18	
Female	27	15	12	NS
Primary site				
Tongue	40	22	18	
Gingiva	14	7	7	
Buccal mucosa	5	2	3	
Hard palate	3	1	2	NS
Histological differentiation				
Well	33	16	17	
Moderately	26	13	13	NS
Poorly	3	3	0	
T classification (extension of primary tumor)[47]				
T1, 2	21	12	9	
T3	17	7	10	
T4	24	13	11	NS
Clinical stage[47]				
I, II	11	9	2	
III	25	11	14	
IV	26	12	14	NS
Histological nodal metastasis[47]				
n–	23	19	4	
n+	39	13	26	0.00018
Disease recurrence				
(–)	35	19	16	
(+)	27	13	14	NS

†Calculated χ^2 test.

To examine the role of HMGB1 in MIA expression in OSCC, we compared the expressions of MIA and HMGB1. HMGB1 immunoreactivity was found in cancer cell nuclei (Fig. 1, HMGB1). MIA grading index was significantly correlated with HMGB1 labeling ($P < 0.0001$) (Fig. 2c).

VEGF-C and VEGF-D were examined as the expressions of lymphangiogenesis -related growth factors in OSCC cases (Fig. 1). We showed comparison between expressions of VEGF-C or VEGF-D and MIA grade or HMGB1 labeling index (Fig. 2d–g). Immunostaining grades of VEGF-C and VEGF-D were correlated with MIA grade ($P < 0.0001$) and HMGB1 labeling index ($P < 0.001$). All above results suggest that MIA is associated with lymph-node metastasis of OSCC by up-regulation of lymphangiogenic factors, VEGF-C and VEGF-D.

Relation of MIA expression with HMGB1 or NFkB p65. We next compared the expression level of MIA, HMGB1 and NFkB p65 in metastatic HSC3 and non-metastatic HSC4 human OSCC cell lines by immunoblotting (Fig. 3). In HSC3 cells, expression levels of MIA, HMGB1 and NFkB p65 were higher than HSC4. U937 monocytic cells, which showed lower HMGB1 and higher NFkBp65 expression levels, expressed MIA at an untraceable level. A physical association between HMGB1 and NFkB p65 was also examined in order to be compared with HMGB1 expression (Fig. 3). The levels of NFkB p65 detected in HMGB1-immunoprecipitants of HSC3 cells were 4.5-times higher than that in HSC4 cells. In U937 cells, NFkB p65 binding with

doi: 10.1111/j.1349-7006.2008.00894.x

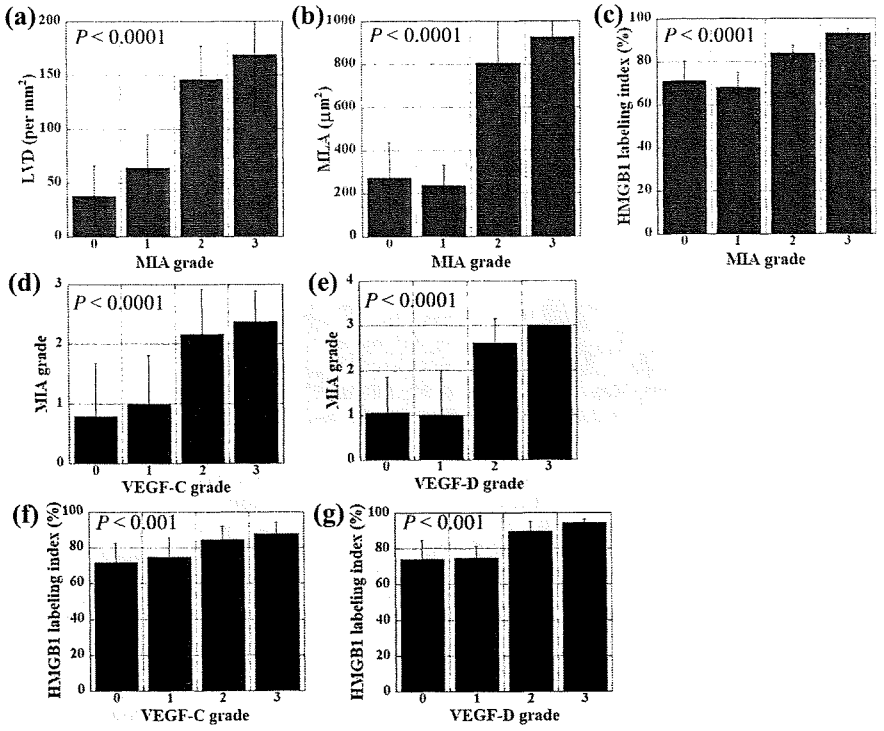

Fig. 2. Relationship between MIA expression and lymph vessels, and expressions of HMGB1, VEGF-C and VEGF-D. MIA grading was compared with lymph vessel density (LVD) (a), mean lymph vessel area (MLA) (b), HMGB1 labeling index (c), VEGF-C grading (d),and VEGF-D grading (e) in OSCC. HMGB1 labeling index was compared with VEGF-C grading (f), and VEGF-D grading (g) in OSCC. Expressions of MIA, VEGF-C, and VEGF-D were categorized according to Allred's score (AS).[30] Grade 0, AS is 0; Grade1, AS is 2-4; Grade 2, AS is 5-6; Grade 3, AS is 7-8. Error bar, SD.

HMGB1 is 1/10 of that in HSC4 cells. HMGB1–NFkB p65 binding levels in HSC3, HSC4 and U937 cells were well correlated with those of MIA expression levels.

Role of HMGB1 on MIA expression in HSC3 OSCC cells. HMGB1 has a dual role as a chromatin structural protein and as a cytokine accelerating macrophage-associated inflammation in cancer growth and invasion. We examined which form of HMGB1 participated in MIA expression (Fig. 4a). Exposure to antisense S-ODN for HMGB1 receptor RAGE did not affect MIA expression levels. The addition of hrHMGB1 into the culture medium also did not affect MIA expression. In contrast, reduction of intracellular protein by HMGB1 antisense S-ODN treatment decreased MIA expression. We confirmed the effects of RAGE and HMGB1 on decreasing the MIA expression by using siRNA for HMGB1 (Fig. 4b,c). RAGE siRNA decreased RAGE mRNA expression, but not MIA mRNA, whereas HMGB1 siRNA decreased HMGB1 and MIA mRNA expression in HSC3 cells. These results suggest that HMGB1 is significant in MIA induction as a transcriptional cofactor with NFkBp65 but not as a RAGE ligand.

MIA intracellular signals and expressions of VEGF-C and VEGF-D. Finally, we examined the MIA effects on HSC3 intracellular signals (Fig. 5). Expressions of VEGF-C and VEGF-D were examined by RT-PCR in HSC3, HSC4 and U937 cells (Fig. 5a). Metastasis-derived HSC3 cells expressed VEGF-C and VEGF-D, whereas original tumor-derived HSC4 cells expressed only VEGF-C. U937 monocytes did not express VEGF-C nor VEGF-D. As shown in Fig. 5(b), inhibiting the expression of MIA secreted by HSC3 cells with anti-MIA antibody increased the phosphorylated form of ERK1/2, whereas phosphorylated p38 was decreased. Expressions of pro-lymphangiogenic growth factors and VEGF-C and VEGF-D were inhibited by MIA neutralization in the antibody treatment. To confirm the relationship of p38 phosphorylation level with VEGF-C or VEGF-D expression, we examined the effect of p38 inihibitor on expression (Fig. 5c). HSC3 cells treated with p38 inhibitor (SB239063) showed decreased expressions of VEGF-C and VEGF-D by RT-PCR examination. Thus, MIA up-regulates VEGF-C and VEGF-D through p38 activation.

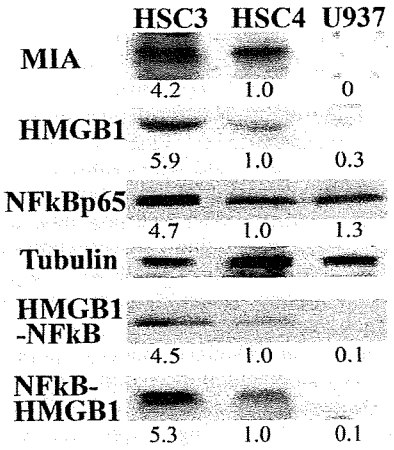

Fig. 3. Expression of melanoma inhibitory activity (MIA), high mobility group box-1 (HMGB1) and nuclear factor kB (NFkB) in human oral squamous cell carcinoma (OSCC) cells. MIA expression was compared with the expressions of HMGB1, NFkBp65 and coprecipitation between NFkBp65 and HMGB1 in HSC3, HSC4 human OSCC cells and U937 monocytic cells. Expressions of MIA, HMGB1 and NFkBp65 were examined by immunoblotting. Tubulin was served as a loading control. Co-precipitation of HMGB1 and NFkB was examined by immunoprecipitation. A precipitant with anti-HMGB1 antibody was detected with anti-NFkBp65 antibody by immunoblotting. Reverse immunoprecipitation was also examined. A precipitant with anti-NFkBp65 antibody was detected with anti-HMGB1 antibody.

Discussion

In the present study, we showed immunoreactivity of MIA was significantly correlated with nodal metastasis, LVD and HMGB1 labeling index in OSCC specimens. In *in vitro* examinations, MIA expression was associated with the expression levels of HMGB1 (not as a cytokine but as an intracellular form) and HMGB1–NFkB p65 binding. In a metastatic OSCC cell line,

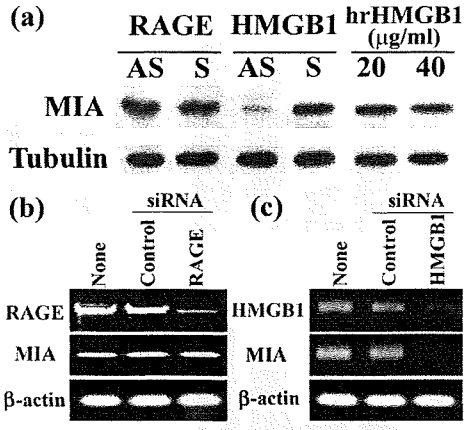

Fig. 4. Effects of antisense S-ODN and siRNA for receptor for advanced glycation end products (RAGE) and high mobility group box-1 (HMGB1) and hrHMGB1 on melanoma inhibitory activity (MIA) expression in HSC3 human oral squamous cell carcinoma (OSCC) cells. (a) MIA expression was examined by immunoblotting in HSC3 human OSCC cells treated with antisense (AS) or sense (S) S-ODN for RAGE and HMGB1 and human recombinant HMGB1 (hrHMGB1). Tubulin was served as a loading control. (b, c) MIA expression was examined by reverse transcriptase–polymerase chain reaction in HSC3 cells with or without treatment with siRNA for RAGE and HMGB1 or control siRNA. β-actin was served as a loading control.

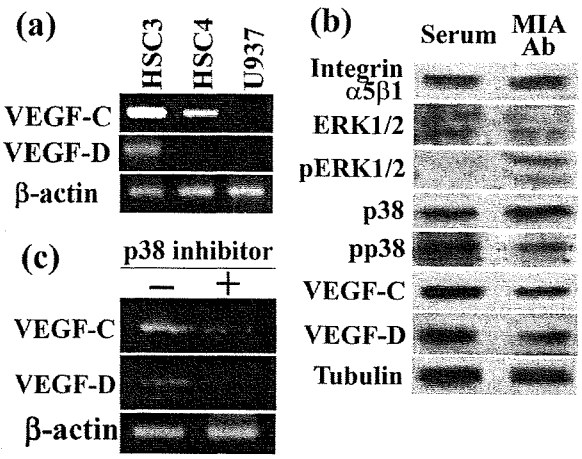

Fig. 5. Melanoma inhibitory activity (MIA) intracellular signaling and vascular endothelial growth factor (VEGF)-C and VEGF-D expression in HSC3 cells. (a) Expression of VEGF-C and VEGF-D was examined by reverse transcriptase–polymerase chain reaction (RT-PCR) in HSC3, HSC4 and U937 cells. β-actin was served as a loading control. (b) Effects of anti-MIA antibody on phosphorylation of extracellular signal-related kinase (ERK)1/2 and p38 and expressions of integrin α5β1, VEGF-C and VEGF-D in HSC3 human oral squamous cell carcinoma (OSCC) cells. Protein levels of MIA, ERK1/2, phosphorylated ERK1/2 (pERK1/2), p38, phosphorylated p38 (pp38), VEGF-C and VEGF-D were examined by immunoblotting in HSC3 human OSCC cells treated with MIA antibody. Tubulin was served as a loading control. (c) The effect of inhibition of p38 on expression of VEGF-C and VEGF-D. HSC3 cells were treated with p38 inhibitor (SB239063). Expression of VEGF-C and VEGF-D was examined by RT-PCR. β-actin was served as a loading control.

HSC3 showed higher MIA expression, which was associated with higher expression levels of HMGB1, NFkB p65 and HMGB1–NFkB p65 binding than those in a non-metastatic OSCC cell line (HSC4). Moreover, MIA expression was associated with VEGF-C and VEGF-D expression in HSC3 cells.

HMGB1 is a chromatin structural protein and also acts as a cytokine or growth factor.[32,33] Nuclear HMGB1 is recruited in gene replication, repair and transcription, whereas secreted HMGB1 worsens endotoxemic inflammation as a late mediator.[33] Secreted HMGB1 is also known as a pro-tumoral factor, as is a RAGE ligand.[34] We reported that co-overexpression of HMGB1 and RAGE is significantly associated with tumor progression and metastasis in gastric cancer,[24] colon cancer,[21,23] prostate cancer[22] and malignant transformation of colorectal adenoma.[35] Further, we found that HMGB1 induces apoptosis of macrophages, which is associated with colon cancer metastasis[25,26] and enhanced extracellular secretion of HMGB1 in colon cancer.[36] We also reported that a high expression level of RAGE is correlated with tumor progression and recurrence, but not with lymph-node metastasis in OSCC.[18–20] RAGE activation with HMGB1 as a ligand induced VEGF expression, but not VEGF-C in HCS3 and HCS4 OSCC cells.[19] In the present study, HMGB1 treatment did not alter MIA expression, whereas HMGB1 antisense S-ODN treatment decreased MIA expression. HMGB1 is able to bind to HCR located in the promoter region of the *MIA* gene where HMGB1 interacts with NFkB p65 to enhance MIA expression transcriptionally.[28,29] In the present study, we confirmed that physical association between HMGB1 and NFkB p65 regulates induction of MIA in OSCC. From these findings, HMGB1 might induce MIA expression acting as a chromosomal protein.

MIA takes a pivotal role for progression and metastasis in melanoma.[12] MIA promotes cell detachment, migration and invasion and inhibits apoptosis of the cancer cells and infiltration of lymphokine activated killer cells (LAK). MIA binds to fibronectin via SH3 domain-like structures, which inhibits cell-to-stromal attachment.[37,38] Further, MIA is able to bind to cell surface integrin α4β1 and α5β1, which suggests MIA might play a role as a ligand for selected integrins.[39]

In the present study, we found a significant relationship between MIA expression and LVD in OSCC tumors. Expression of integrin α5β1 in lymph vessel endothelial cells is associated with outgrowth of new lymphatic vessels.[40] MIA might stimulate lymphatic endothelial cells directly to induce lymphangiogenesis. We also found a relationship between MIA expression and VEGF-C and VEGF-D expression in HSC-3 OSCC cells, which expressed integrin α5β1. MAPK activity is reported to be affected by MIA,[39] which we confirmed in the present study. ERK1/2 phosphorylation was recovered by MIA neutralization by the antibody treatment. In contrast, p38 phosphorylation levels were decreased by the antibody treatment. VEGF-C expression is inhibited by p38 inhibitor but not by ERK1/2 inhibitor.[41] We also confirmed the significance of p38 activation on up-regulation of VEGF-C and -D in HSC3 cells. The alteration of the signal balance between ERK1/2 and p38 might be associated with up-regulation of VEGF-C and -D expression by MIA. Further examination will reveal the details of the mechanism of MIA-dependent VEGF-C and -D induction. VEGF-C and -D are known as strong lymphangiogenic factors in various cancers.[42] Increased VEGF-C expression is associated with cervical lymph-node metastasis in head and neck cancer.[43] Although there are still controversies about the role of VEGF-D in lymph-node metastasis, VEGF-D expression is also associated with lymph-node metastasis in the animal model.[44] Our data suggest that up-regulation of VEGF-C and -D might explain the relationship between MIA expression and lymph-node metastasis in OSCC.

HSC3 cells are tongue squamous cell carcinoma-derived metastatic cell lines, which provide many sublines with high metastatic potential. In contrast, HSC4 cells show low metastatic potential. No metastatic sublines are derived from HSC4 cells.[45] Metastatic HSC3 cells show colony formation in the type-I collagen matrix, adherence to type-IV collagen,[45] high heparanase activity[31] and reduced nm23H1 expression and up-regulated matrix metalloproteinase (MMP)-2 and -9[46] in

doi: 10.1111/j.1349-7006.2008.00894.x

comparison with HSC4 cells. In the present study, HSC3 cells showed overexpression of MIA, HMGB1, NFkBp65, VEGF-C and VEGF-D in comparison with HSC4 cells. Thus the increase of lymphangiogenic capacity might be associated with high potential of lymph-node metastasis in HSC3. Further examination of the lymphangiogenic capacity might control lymph-node metastasis in OSCC. In the present study, MIA expression was associated with a high incidence of lymph-node metastasis, whereas MIA expression did not correlate with recurrence nor with disease-free survival. Our previous data show that RAGE–HMGB1 coexpression is associated with T classification (extension of primary tumor) but not nodal metastasis in OSCC; however, RAGE expression is closely associated with recurrence and disease-free survival.[18–20] Many OSCC recurred at the local sites but not from nodal metastasis (data not shown). Local recurrence of OSCC depends on aggressiveness of cancer invasion and anatomical difficulties in the head to obtain sufficient surgical margins. In OSCC, both metastatic potential and local aggressiveness are significant factors to determine the disease outcome.

We showed that MIA was expressed in more than 60% of metastasized OSCC. Considering MIA is a secretory protein, MIA might be a useful marker for metastasis of OSCC, which is detectable in the serum and saliva of OSCC patients. Further examination of MIA might be expected to provide a new target for suppression of lymph-node metastasis.

Acknowledgments

This work was supported in part by Grant-in-Aid for Scientific Research from the Japan Society for the Promotion of Science, Japan. The authors thank Ms Kaori Isobe for expert assistance with the preparation of this manuscript.

References

1 Paterson IC, Eveson JW, Prime SS. Molecular changes in oral cancer may reflect aetiology and ethnic origin. *Eur J Cancer B Oral Oncol* 1996; **32B**: 150–3.
2 Chen YJ, Lin SC, Kao T *et al.* Genome-wide profiling of oral squamous cell carcinoma. *J Pathol* 2004; **204**: 326–32.
3 Hunter KD, Parkinson EK, Harrison PR. Profiling early head and neck cancer. *Nat Rev Cancer* 2005; **5**: 127–35.
4 Woolgar JA, Rogers S, West CR, Errington RD, Brown JS, Vaughan ED. Survival and patterns of recurrence in 200 oral cancer patients treated by radical surgery and neck dissection. *Oral Oncol* 1999; **35**: 257–65.
5 Lippman SM, Hong WK. Molecular markers of the risk of oral cancer. *N Engl J Med* 2001; **344**: 1323–6.
6 Hershkovich O, Oliva J, Nagler RM. Lethal synergistic effect of cigarette smoke and saliva in an *in vitro* model: does saliva have a role in the development of oral cancer? *Eur J Cancer* 2004; **40**: 1760–7.
7 Blesch A, Bosserhoff AK, Apfel R *et al.* Cloning of a novel malignant melanoma-derived growth-regulatory protein, MIA. *Cancer Res* 1994; **54**: 5695–701.
8 Bosserhoff AK, Hein R, Bogdahn U, Buettner R. Structure and promoter analysis of the gene encoding the human melanoma-inhibiting protein MIA. *J Biol Chem* 1996; **271**: 490–5.
9 Koehler MR, Bosserhoff A, von Beust G *et al.* Assignment of the human melanoma inhibitory activity gene (MIA) to 19q13.32-q13.33 by fluorescence *in situ* hybridization (FISH). *Genomics* 1996; **35**: 265–7.
10 Bosserhoff AK, Moser M, Hein R, Landthaler M, Buettner R. *In situ* expression patterns of melanoma-inhibiting activity (MIA) in melanomas and breast cancers. *J Pathol* 1999; **187**: 446–54.
11 Poser I, Tatzel J, Kuphal S, Bosserhoff AK. Functional role of MIA in melanocytes and early development of melanoma. *Oncogene* 2004; **23**: 6115–24.
12 Bosserhoff AK, Kaufmann M, Kaluza B *et al.* Melanoma-inhibiting activity, a novel serum marker for progression of malignant melanoma. *Cancer Res* 1997; **57**: 3149–53.
13 Bosserhoff AK, Kondo S, Moser M *et al.* Mouse CD-RAP/MIA gene: structure, chromosomal localization, and expression in cartilage and chondrosarcoma. *Dev Dyn* 1997; **208**: 516–25.
14 Hau P, Ruemmele P, Kunz-Schughart LA *et al.* Expression levels of melanoma inhibitory activity correlate with time to progression in patients with high-grade glioma. *Oncol Rep* 2004; **12**: 1355–64.
15 El Fitori J, Kleeff J, Giese NA *et al.* Melanoma inhibitory activity (MIA) increases the invasiveness of pancreatic cancer cells. *Cancer Cell Int* 2005; **5**: 3.
16 Lee KL, Pentecost BT, D'Anna JA, Tobey RA, Gurley LR, Dixon GH. Characterization of cDNA sequences corresponding to three distinct HMG-1 mRNA species in line CHO Chinese hamster cells and cell cycle expression of the *HMG-1* gene. *Nucleic Acids Res* 1987; **15**: 5051–68.
17 Rauvala H, Pihlaskari R. Isolation and some characteristics of an adhesive factor of brain that enhances neurite outgrowth in central neurons. *J Biol Chem* 1987; **262**: 16625–35.
18 Sasahira T, Kirita T, Bhawal UK *et al.* Expression of receptor for advanced glycation end products (RAGE) is associated with angiogenesis in human oral squamous cell carcinoma. *Virchows Arch* 2007; **450**: 287–95.
19 Sasahira T, Kirita T, Bhawal UK, Yamamoto K, Kuniyasu H. Significance of expression of receptor for advanced glycation end products (RAGE) in recurrence of human oral squamous cell carcinoma. *Histopathol* 2007; **51**: 166–72.
20 Bhawal UK, Ozaki Y, Nishimura M *et al.* Association of expression of receptors for advanced glycation end-products (RAGE) and invasive and metastatic activity of oral squamous cell carcinoma. *Oncology* 2005; **69**: 246–55.
21 Kuniyasu H, Chihara Y, Kondo H. Differential effects between amphoterin and advanced glycation end products on colon cancer cells. *Int J Cancer* 2003; **104**: 722–7.
22 Kuniyasu H, Chihara Y, Kondo H, Ohmori H, Ukai R. Amphoterin induction in prostatic stromal cells by androgen deprivation is associated with metastatic prostate cancer. *Oncol Rep* 2003; **10**: 1863–8.
23 Kuniyasu H, Chihara Y, Takahashi T. Co-expression of receptor for advanced glycation end products and the ligand amphoterin associates closely with metastasis of colorectal cancer. *Oncol Rep* 2003; **10**: 445–8.
24 Kuniyasu H, Oue N, Wakikawa A *et al.* Expression of receptors for advanced glycation end-products (RAGE) is closely associated with the invasive and metastatic activity of gastric cancer. *J Pathol* 2002; **196**: 163–70.
25 Kuniyasu H, Sasaki T, Sasahira T, Ohmori H, Takahashi T. Depletion of tumor-infiltrating macrophages is associated with amphoterin expression in colon cancer. *Pathobiology* 2004; **71**: 129–36.
26 Kuniyasu H, Yano S, Sasaki T, Sasahira T, Sone S, Ohmori H. Colon cancer cell-derived high mobility group 1/amphoterin induces growth inhibition and apoptosis in macrophages. *Am J Pathol* 2005; **166**: 751–60.
27 Stros M, Ozaki T, Bacikova A, Kageyama H, Nakagawara A. HMGB1 and HMGB2 cell-specifically down-regulate the p53- and p73-dependent sequence-specific transactivation from the human Bax gene promoter. *J Biol Chem* 2002; **277**: 7157–64.
28 Poser I, Golob M, Buettner R, Bosserhoff AK. Upregulation of HMG1 leads to melanoma inhibitory activity expression in malignant melanoma cells and contributes to their malignancy phenotype. *Mol Cell Biol* 2003; **23**: 2991–8.
29 Golob M, Buettner R, Bosserhoff AK. Characterization of a transcription factor binding site, specifically activating MIA transcription in melanoma. *J Invest Dermatol* 2000; **115**: 42–7.
30 Allred DC, Harvey JM, Berardo M, Clark GM. Prognostic and predictive factors in breast cancer by immunohistochemical analysis. *Mod Pathol* 1998; **11**: 155–68.
31 Ikuta M, Podyma KA, Maruyama K, Enomoto S, Yanagishita M. Expression of heparanase in oral cancer cell lines and oral cancer tissues. *Oral Oncol* 2001; **37**: 177–84.
32 Parkkinen J, Raulo E, Merenmies J *et al.* Amphoterin, the 30-kDa protein in a family of HMG1-type polypeptides. Enhanced expression in transformed cells, leading edge localization, and interactions with plasminogen activation. *J Biol Chem* 1993; **268**: 19726–38.
33 Czura CJ, Wang H, Tracey KJ. Dual roles for HMGB1: DNA binding and cytokine. *J Endotoxin Res* 2001; **7**: 315–21.
34 Taguchi A, Blood DC, del Toro G *et al.* Blockade of RAGE-amphoterin signalling suppresses tumour growth and metastases. *Nature* 2000; **405**: 354–60.
35 Sasahira T, Akama Y, Fujii K, Kuniyasu H. Expression of receptor for advanced glycation end products and HMGB1/amphoterin in colorectal adenomas. *Virchows Arch* 2005; **446**: 411–5.
36 Sasahira T, Sasaki T, Kuniyasu H, Akama Y, Fujii K. Interleukin-15 and transforming growth factor alpha are associated with depletion of tumor-associated macrophages in colon cancer. *J Exp Clin Cancer Res* 2005; **24**: 69–74.
37 Bosserhoff AK, Stoll R, Sleeman JP, Bataille F, Buettner R, Holak TA. Active detachment involves inhibition of cell-matrix contacts of malignant melanoma cells by secretion of melanoma inhibitory activity. *Lab Invest* 2003; **83**: 1583–94.
38 Jachimczak P, Apfel R, Bosserhoff AK *et al.* Inhibition of immunosuppressive effects of melanoma-inhibiting activity (MIA) by antisense techniques. *Int J Cancer* 2005; **113**: 88–92.

39 Bauer R, Humphries M, Faessler R, Winklmeier A, Craig SE, Bosserhoff AK. Regulation of integrin activity by MIA. *J Biol Chem* 2006; **281**: 11669–77.
40 Dietrich T, Onderka J, Bock F *et al.* Inhibition of inflammatory lymphangiogenesis by integrin alpha5 blockade. *Am J Pathol* 2007; **171**: 361–72.
41 Kobayashi S, Kishimoto T, Kamata S, Otsuka M, Miyazaki M, Ishikura H. Rapamycin, a specific inhibitor of the mammalian target of rapamycin, suppresses lymphangiogenesis and lymphatic metastasis. *Cancer Sci* 2007; **98**: 726–33.
42 Stacker SA, Achen MG, Jussila L, Baldwin ME, Alitalo K. Lymphangiogenesis and cancer metastasis. *Nat Rev Cancer* 2002; **2**: 573–83.
43 O-charoenrat P, Rhys-Evans P, Eccles SA. Expression of vascular endothelial growth factor family members in head and neck squamous cell carcinoma correlates with lymph node metastasis. *Cancer* 2001; **92**: 556–68.
44 Stacker SA, Caesar C, Baldwin ME *et al.* VEGF-D promotes the metastatic spread of tumor cells via the lymphatics. *Nat Med* 2001; **7**: 186–91.
45 Momose F, Araida T, Negishi A, Ichijo H, Shioda S, Sasaki S. Variant sublines with different metastatic potentials selected in nude mice from human oral squamous cell carcinomas. *J Oral Pathol Med* 1989; **18**: 391–5.
46 Khan MH, Yasuda M, Higashino F, Haque S, Kohgo T, Nakamura M, Shindoh M. nm23-H1 suppresses invasion of oral squamous cell carcinoma-derived cell lines without modifying matrix metalloproteinase-2 and matrix metalloproteinase-9 expression. *Am J Pathol* 2001; **158**: 1785–91.
47 Fleming ID, Cooper JS, Henson DE *et al. AJCC Cancer Staging Manual.* Lippincott-Raven, Philadelphia, 1997.

doi: 10.1111/j.1349-7006.2008.00894.x

Positive immunohistochemical staining of γH2AX is associated with tumor progression in gastric cancers from radiation-exposed patients

KAZUHIRO SENTANI[1], NAOHIDE OUE[1], NAOYA SAKAMOTO[1], TAKASHI NISHISAKA[2], TOSHIYUKI FUKUHARA[2], HIROO MATSUURA[3] and WATARU YASUI[1]

[1]Department of Molecular Pathology, Hiroshima University Graduate School of Biomedical Sciences, Hiroshima; [2]Department of Pathology and Laboratory Medicine, Hiroshima Prefectural Hospital, Hiroshima; [3]Department of Pathology, Hiroshima City Hospital, Hiroshima, Japan

Received May 27, 2008; Accepted August 2, 2008

DOI: 10.3892/or_00000120

Abstract. To elucidate the mechanism of radiation-induced cancers, molecular analysis of cancers in atomic bomb (A-bomb) exposure is important. DNA double-strand breaks (DSBs) are thought to be caused by the deleterious effects of ionizing radiation, and γH2AX (serine 139 phosphorylated form of histone H2AX) is reported to be a significant marker for DSBs. In the present study, we performed immunohistochemical analysis of γH2AX in gastric cancers (GCs) from 66 exposed and 47 non-exposed patients who developed GC after the bombing. Of the 47 GCs from non-exposed patients, 6 (13%) cases showed nuclear positive staining for γH2AX, whereas of the 66 GCs from exposed patients, 20 (30%) cases were positive (P=0.0405). However, among stage I GC, there was no significant difference in γH2AX expression frequency between exposed patients and non-exposed patients. Among exposed patients, stage II-IV cases were more frequently positive for γH2AX than stage I cases (P=0.0197). Among GCs from non-exposed patients, γH2AX staining showed no significant association with Lauren's classification, depth of invasion, lymph node metastasis or TNM stage. These results suggest that the characteristics of tumor cells differ between GCs from exposed and non-exposed patients. DSBs may be involved in progression of GC in exposed patients.

Introduction

More than 60 years have passed since atomic bomb (A-bombs) exposure in Hiroshima and Nagasaki, Japan. A prospective cohort study (Life Span Study, LSS) of 120,000 subjects is being conducted by the Radiation Effects Research Foundation (RERF) (1). It was reported that exposure to ionizing radiation (IR) increases the risk of leukemia and other cancers (2), and damage to nuclear DNA likely represents an initiating event for carcinogenesis. Increases in cancer risk due to exposure to IR are based on epidemiologic studies of exposed human populations, mainly the A-bomb survivors of Hiroshima and Nagasaki (3). Solid cancers, including breast, colon, lung and stomach cancers, have a long latency period, and the excess relative risks (RRs) of solid cancers remain high, specifically among those exposed when young (1). Although approximately half of the LSS members are now deceased, cancer mortality in the LSS has continued to increase as this population ages, and it is anticipated to peak in 2015.

According to the World Health Organization, gastric cancer (GC) is the fourth most common malignancy worldwide, with approximately 870,000 new cases occurring yearly. Cancer develops as a result of multiple genetic and epigenetic alterations (4,5). Although several genetic alterations, including mutations in *TP53* and *BRAF*, have been reported in selected cancers of A-bomb survivors (6-8), specific mutations for radiation-associated cancers have not been reported.

DNA double-strand breaks (DSBs) are thought to be caused by the deleterious effects of IR (9,10). DSBs can induce chromosomal aberrations that cause cells to malfunction, resulting in cell death or tumorigenesis (10). One of the earliest steps in the cellular response to DSBs is the phosphorylation of histone H2AX at serine 139 (γH2AX), the site of γ-phosphorylation (11). H2AX can be phosphorylated by several phosphoinositide-3 (PI3) kinases including ataxia telangiectasia mutated (ATM), DNA-dependent protein kinase (DNA-PK) and ataxia telangiectasia and Rad3 related (ATR) (12). The number of resulting γH2AX foci has been correlated directly with the number of DSBs produced by IR (13,14). Therefore, the number of γH2AX foci is a significant marker for DSBs. Immunohistochemical analyses of γH2AX have been reported for human cancers of the urinary bladder,

Correspondence to: Dr Wataru Yasui, Department of Molecular Pathology, Hiroshima University Graduate School of Biomedical Sciences, 1-2-3 Kasumi, Minami-ku, Hiroshima 734-8551, Japan
E-mail: wyasui@hiroshima-u.ac.jp

Key words: γH2AX, gastric cancer, radiation, atomic bomb, DNA double-strand break

breast, lung, colon and prostate (15-17). It was also reported that γH2AX-positive cells are present in colorectal cancer (CRC) and precursor lesions, such as adenoma, but not in normal colonic epithelium (15). Furthermore, invasive CRCs were reported to show less γH2AX staining than adenomas (15). These results suggest that staining of γH2AX correlates with DNA damage checkpoint activation in premalignant lesions. Therefore, the existence of γH2AX foci might be a useful and sensitive marker of cancer, especially for detecting cancers or precursor lesions in A-bomb survivor, because IR induces DSBs. However, there are no reports of immunohistochemical analyses of γH2AX in GCs from either IR-exposed patients or -non-exposed patients. Therefore, in the present study, we performed immunohistochemical analysis of γH2AX in 113 GCs derived from A-bomb survivors.

Patients and methods

Patients and tumor specimens. For immunohistochemical analysis, we used formalin-fixed, paraffin-embedded archival tissues from 113 patients with GC who underwent surgery between 1975 and 2005 at Hiroshima University Hospital (Hiroshima, Japan) or an affiliated hospital. Only patients who did not undergo preoperative radio- or chemotherapy were enrolled in the study. All 113 patients were A-bomb survivors (LSS cohort members) in Hiroshima, Japan. Although these patients were survivors who developed GC after the bombing, they were further classified according to their level of radiation exposure (i.e., ≥5 mGy and <5 mGy were defined as 'exposed' and 'non-exposed', respectively). Our population comprised 66 exposed (median dose, 51 mGy; range, 5-2601 mGy) and 47 non-exposed patients (median dose, 0 mGy; range, 0-4 mGy).

Tumor staging was performed according to the Union Internationale Contre le Cancer (UICC) system (18). Histologic classification was carried out according to the Lauren classification system (19). The detailed procedures for acquiring informed consent from study patients and collecting tissue specimens were described previously (20). In accordance with the Ethical Guidelines For Human Genome/Gene Research enacted by the Japanese Government, tissue specimens were collected and used after approval from the Ethical Review Committee of the Hiroshima University School of Medicine and from the ethical review committees of collaborating organizations.

Radiation dose. A-bomb radiation doses were estimated with the DS02 system (21).

Immunohistochemistry. From each patient, one representative tumor block, including the tumor center and invasive front as well as tumor-associated non-neoplastic mucosa, was examined by immunohistochemistry. In cases of large, late-stage tumors, different sections were examined to include representative areas of the tumor center as well as of the lateral and deep tumor invasive fronts.

Immunohistochemical detection of γH2AX was performed with a mouse monoclonal antibody (Upstate Biotechnology, Chicago, IL, USA) and Dako Envision Kit (Dako, Carpinteria, CA). In brief, sections were pretreated by microwaving (500 W) in citrate buffer (pH 6.0) for 15 min to retrieve antigenicity. After endogenous peroxidase activity was blocked with 3% H_2O_2-methanol for 10 min, sections were incubated with normal goat serum (Dako) for 20 min to block non-specific antibody binding sites. Sections were then incubated with anti-γH2AX (diluted 1:200) for 1 h at room temperature followed by incubation with peroxidase-labelled anti-mouse IgG for 60 min. Staining was completed with a 10-min incubation with the substrate-chromogen solution. Sections were counterstained with 0.1% hematoxylin. Appropriate negative controls were created by omission of the primary antibody. All slices were evaluated without knowledge of the clinical data.

Double immunofluorescence staining. Double immunofluorescence staining for dewaxed sections was performed with mouse monoclonal anti-γH2AX antibody (Upstate) with rabbit polyclonal anti-H2AX antibody (Upstate) or mouse monoclonal anti-γH2AX antibody with a rabbit polyclonal antibody against the activated form of caspase-3 (Promega, Madison, WI, USA). Microwave pretreatment in citrate buffer was performed for 15 min to retrieve antigenicity. Sections were then incubated with normal goat serum for 30 min to block non-specific antibody binding sites. Sections were treated consecutively at room temperature with primary antibodies for 60 min, and immunocomplexes were detected with Alexa Fluor 488-conjugated goat anti-mouse IgG and Alexa Fluor 546-conjugated goat anti-rabbit IgG (Molecular Probes, Eugene, OR, USA).

Statistical methods. Associations between clinicopathologic variables and immunostaining for γH2AX were analyzed by Fisher's exact test. A P-value <0.05 was considered statistically significant.

Results

Of 113 GC from A-bomb survivors, 48 (42%) showed nuclear staining of γH2AX (Fig. 1A). These 48 cases comprised 26 GC cases with diffuse staining for γH2AX and 22 GC cases with staining of γH2AX only in superficial portions (Fig. 1B) or in necrotic debris in the lumen (Fig. 1C). We confirmed that γH2AX yielded granular, nuclear staining (Fig. 1D). H2AX showed ubiquitous staining in GC (Fig. 1E). It was reported previously that γH2AX is expressed during early apoptosis triggered through the caspase-3/caspase-activated DNase (CAD) pathway (22,23). Double immunofluorescence staining revealed that γH2AX-positive tumor cells in superficial portions or necrotic debris were also positive for the activated form of caspase-3 (a marker of apoptosis) (Fig. 1F). Because we believed that γH2AX staining induced by apoptosis was not related to IR, cases with superficial staining and staining of necrotic debris were excluded from the positive cases. In contrast, the percentage of γH2AX-stained tumor cells was >5% in 26 GC cases showing diffuse staining; we considered these as positive cases. Twenty-four of 26 GC cases had from 5% to 10% of γH2AX-stained tumor cells. In particular, remaining two cases had >30% of γH2AX-stained tumor cells, both of which were α-fetoprotein (AFP)-positive GC.

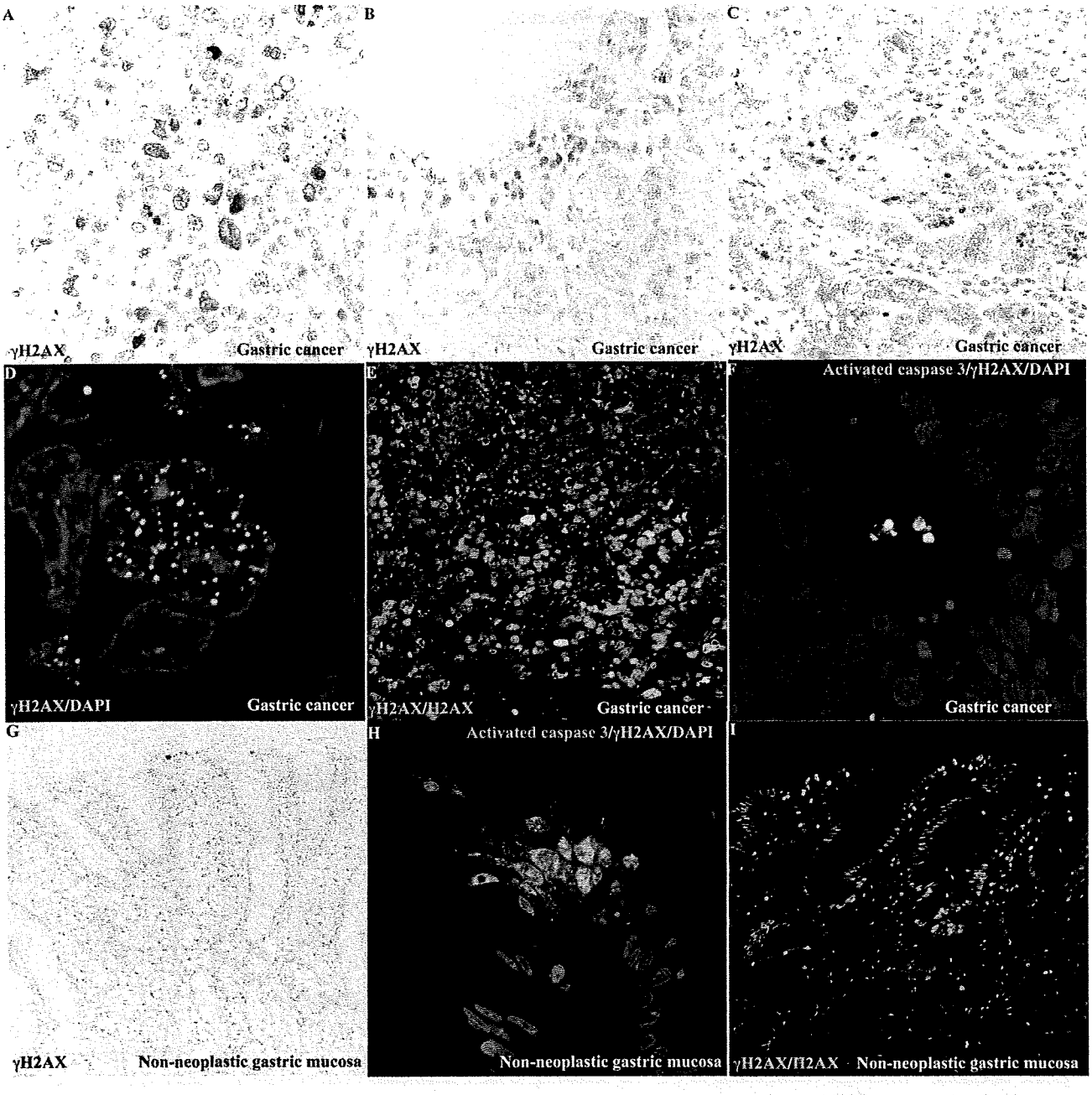

Figure 1. Immunohistochemical analysis of γH2AX in gastric carcinoma (GC) tissues (A-F) and non-neoplastic gastric mucosa (G-I). Staining for γH2AX in GC. Schematic representation of a positive case (A). Tumor cells or necrotic debris with γH2AX staining are located at the superficial portion of GCs (B) or in the lumen of the tumor gland (C). Granular staining of γH2AX is found in the nucleus (D). Staining for H2AX. H2AX shows ubiquitous staining both in GC (E) and non-neoplastic gastric mucosa (I). Some surface cells in non-neoplastic gastric mucosa also express γH2AX (G). Double immunofluorescence staining of the activated form of caspase-3 and γH2AX. Necrotic debris in the lumen of GCs (F) and superficial apoptotic cells in non-neoplastic gastric mucosa (H) are shown. Cells were imaged with a fluorescence microscope as described in Materials and methods.

We analyzed the association between γH2AX staining and clinicopathologic parameters in GCs from 66 IR exposed and 47 non-exposed patients (Table I). When all tumor stages were considered, γH2AX staining was detected in 20 (30%) of 66 exposed patients and 6 (13%) of 47 non-exposed patients (P=0.0405). Because IR is a carcinogen and can increase an individual's risk of tumor development, we analyzed immunohistochemical staining for γH2AX in early-stage GCs. In GCs showing T1 (tumor invades lamina propria or submucosa), N0 (no regional lymph node metastasis), or stage I, γH2AX positivity did not differ significantly between exposed and non-exposed patients. In contrast, among T2-4 GCs, γH2AX was expressed more often in exposed patients than in non-exposed patients (P=0.0236). In stage II-IV GCs, γH2AX expression showed a marginally significant difference between exposed patients and non-exposed patients (P=0.0602).

Of the 66 GCs from exposed patients, γH2AX was present in 20 (30%). γH2AX expression in GCs from exposed patients was associated significantly with depth of invasion (P=0.003) (Table II). Furthermore, γH2AX staining was observed more frequently in stage II-IV GCs than in stage I GCs (P=0.0197) (Table II). In contrast, the presence of γH2AX in GCs from non-exposed patients showed no signi-

Table I. Expression of γH2AX in GC and its association with clinicopathologic variables.

	No. of cases	γH2AX positive (%)	P-value
GC	113	26 (23)	
Exposed patients	66	20 (30)	
Non-exposed patients	47	6 (13)	0.0405
Intestinal type[a]			
Exposed patients	34	9 (26)	
Non-exposed patients	33	5 (15)	0.3689
Diffuse type[a]			
Exposed patients	32	11 (34)	
Non-exposed patients	14	1 (7)	0.073
Depth of invasion[b]			
T1			
Exposed patients	15	0 (0)	
Non-exposed patients	19	2 (11)	0.492
T2-4			
Exposed patients	51	20 (39)	
Non-exposed patients	28	4 (14)	0.0236
Lymph node metastasis[b]			
N0			
Exposed patients	25	5 (20)	
Non-exposed patients	24	2 (8)	0.4174
N1-4			
Exposed patients	41	15 (37)	
Non-exposed patients	23	4 (17)	0.1552
TNM stage[b]			
I			
Exposed patients	21	2 (10)	
Non-exposed patients	23	2 (9)	1.000
II-IV			
Exposed patients	45	18 (40)	
Non-exposed patients	24	4 (17)	0.0602

GC, gastric carcinoma. [a]Histologic classification of GC was according to the Lauren classification system. [b]Tumor stage was according to the Tumor-Node-Metastasis (TNM) staging system.

ficant correlation with Lauren's classification, depth of invasion, lymph node metastasis or TNM stage (Table II). There was no significant association between γH2AX staining and radiation dose at the time of A-bombing (data not shown).

In non-neoplastic gastric mucosa or intestinal metaplasia adjacent to the tumor, only a few superficial cells in both exposed and non-exposed patients showed immunostaining of γH2AX (Fig. 1G) and activated form of caspase-3 (Fig. 1H). H2AX showed ubiquitous immunostaining (Fig. 1I).

Discussion

While the DNA damage response plays a major role in tumor suppression, how this response contributes to suppression of stomach tumorigenesis remains unclear. DSBs of chromosomal DNA are thought to be caused by the hazardous effects of IR and may result in chromosomal translocations, deletions or loss of genetic information, which are all causatively linked to tumorigenesis (15). Therefore, DSBs may be involved in radiation-associated gastric carcinogenesis among A-bomb survivors. In the present study, we provide immunohistochemical evidence that γH2AX is expressed in 13% of GCs from non-exposed patients and 30% of GCs from exposed patients. Because IR is a carcinogen and can increase an individual's risk of tumor development, DSBs appear to play a more important role in early-stage GC rather than late-stage GC. In fact, γH2AX is reported to be expressed commonly in early precursor lesions in urinary bladder, breast, lung, colon and prostate (15,17). However, in

Table II. Immunohistochemical analysis of γH2AX in GCs from exposed and non-exposed patients.

	No. of cases	γH2AX positive (%)	P-value
Exposed GC patients	66	20 (30)	
Histology[a]			
Intestinal type	34	9 (26)	
Diffuse type	32	11 (34)	0.5946
Depth of invasion[b]			
T1	15	0 (0)	
T2-4	51	20 (39)	0.003
Lymph node metastasis[b]			
N0	25	5 (20)	
N1-4	41	15 (37)	0.1792
TNM stage[b]			
I	21	2 (10)	
II-IV	45	18 (40)	0.0197
Non-exposed GC patients	47	6 (13)	
Histology[a]			
Intestinal type	33	5 (15)	
Diffuse type	14	1 (7)	0.6532
Depth of invasion[b]			
T1	19	2 (11)	
T2-4	28	4 (14)	1.000
Lymph node metastasis[b]			
N0	24	2 (8)	
N1-4	23	4 (17)	0.4158
TNM stage[b]			
I	23	2 (9)	
II-IV	24	4 (17)	0.6662

GC, gastric carcinoma. [a]Histologic classification of GC was according to the Lauren classification system. [b]Tumor stage was done according to be the Tumor-Node-Metastasis (TNM) staging system.

the present study, there was no significant difference in γH2AX staining between stage I GCs from exposed patients and non-exposed patients. Furthermore, in intestinal metaplasia adjacent to the tumor, which is considered to be a gastric precancerous lesion, staining of γH2AX was not observed in epithelial or stromal cells. These results suggest that DSBs are less likely to be involved in the genesis of GCs.

In contrast, in exposed patients, γH2AX-positive GC cases showed more advanced depth of invasion and higher TNM stage than γH2AX-negative GC cases, suggesting that DSBs may participate in progression of GC in exposed patients. It has been reported that deregulated c-myc expression induces DNA damage and the formation of γH2AX (24). However, mammalian SWI/SNF complexes facilitate DSBs repair by promoting γH2AX product (25), and we reported previously that increased expression of BRG1, a component of the SWI/SNF complex, is associated with advanced-stage GCs (26). It is possible that such signals may also contribute to γH2AX activation in GCs from exposed patients. Taken together, the molecular mechanisms that underlie phosphorylation of γH2AX may differ between IR-exposed patients and -non-exposed patients. It is also possible that because a single DSB can result in chromosomal translocations, deletions or loss of genetic information, several genes associated with tumor progression may be deleted in γH2AX-positive GC cases. Further studies are needed to identify these mechanisms.

In conclusion, DSBs do not appear to be characteristic alterations in stomach carcinogenesis in IR-exposed patients. However, immunohistochemical staining of γH2AX is increased with tumor progression in GCs from exposed patients. Although it is unclear whether all GCs from exposed patients in the present study were radiation-induced cancers, DSBs may serve as a marker for progression of GCs.

Acknowledgements

We thank Ms. Emiko Hisamoto for excellent technical assistance and advice. This work was carried out with the kind cooperation of the Research Center for Molecular Medicine, Faculty of Medicine, Hiroshima University. We thank the Analysis Center of Life Science, Hiroshima University for the use of their facilities. This work was supported, in part, by Grants-in-Aid for Cancer Research from the Ministry of Education, Culture, Science, Sports, and Technology of Japan; in part by a Grant-in-Aid for the Third Comprehensive 10-Year Strategy for Cancer Control and for Cancer Research from the Ministry of Health, Labour and Welfare of Japan.

References

1. Preston DL, Ron E, Tokuoka S, *et al*: Solid cancer incidence in atomic bomb survivors: 1958-1998. Radiat Res 168: 1-64, 2007.
2. Yiin JH, Schubauer-Berigan MK, Silver SR, *et al*: Risk of lung cancer and leukemia from exposure to ionizing radiation and potential confounders among workers at the Portsmouth Naval Shipyard. Radiat Res 163: 603-613, 2005.
3. Ron E, Preston DL, Mabuchi K, Thompson DE and Soda M: Cancer incidence in atomic bomb survivors. Part IV: comparison of cancer incidence and mortality. Radiat Res 137: 98-112, 1994.
4. Yasui W, Oue N, Kitadai Y and Nakayama H: Recent advances in molecular pathobiology of gastric carcinoma. In: The Diversity of Gastric Carcinoma Pathogenesis: Diagnosis and Therapy. Kaminishi M, Takubo K and Mafune K (eds). Springer, Tokyo, pp51-71, 2005.
5. Ushijima T and Sasako M: Focus on gastric cancer. Cancer Cell 5: 121-125, 2004.
6. Takeshima Y, Seyama T, Bennett WP, *et al*: p53 mutations in lung cancers from non-smoking atomic-bomb survivors. Lancet 342: 1520-1521, 1993.
7. Takahashi K, Eguchi H, Arihiro K, *et al*: The presence of BRAF point mutation in adult papillary thyroid carcinomas from atomic bomb survivors correlates with radiation dose. Mol Carcinog 46: 242-248, 2007.
8. Iwamoto KS, Mizuno T, Tokuoka S, Mabuchi K and Seyama T: Frequency of p53 mutations in hepatocellular carcinomas from atomic bomb survivors. J Natl Cancer Inst 90: 1167-1168, 1998.
9. Hoeijmakers JH: Genome maintenance mechanisms for preventing cancer. Nature 411: 366-374, 2001.
10. Van Gent DC, Hoeijmakers JH and Kanaar R: Chromosomal stability and the DNA double-stranded break connection. Nat Rev Genet 2: 196-206, 2001.
11. Rogakou EP, Pilch DR, Orr AH, Ivanova VS and Bonner WM: DNA double-stranded breaks induce histone H2AX phosphorylation on serine 139. J Biol Chem 273: 5858-5868, 1998.
12. Paull TT, Rogakou EP, Yamazaki V, Kirchgessner CU, Gellert M and Bonner WM: A critical role for histone H2AX in recruitment of repair factors to nuclear foci after DNA damage. Curr Biol 10: 886-895, 2000.
13. Rothkamm K and Lobrich M: Evidence for a lack of DNA double-strand break repair in human cells exposed to very low x-ray doses. Proc Natl Acad Sci USA 100: 5057-5062, 2003.
14. Sedelnikova OA, Rogakou EP, Panyutin IG and Bonner WM: Quantitative detection of (125)IdU-induced DNA double-strand breaks with gamma-H2AX antibody. Radiat Res 158: 486-492, 2002.
15. Bartkova J, Horejsi Z, Koed K, *et al*: DNA damage response as a candidate anti-cancer barrier in early human tumorigenesis. Nature 434: 864-870, 2005.
16. Gorgoulis VG, Vassiliou LV, Karakaidos P, *et al*: Activation of the DNA damage checkpoint and genomic instability in human precancerous lesions. Nature 434: 907-913, 2005.
17. Fan C, Quan R, Feng X, *et al*: ATM activation is accompanied with earlier stages of prostate tumorigenesis. Biochim Biophys Acta 1763: 1090-1097, 2006.
18. Sobin LH, Wittekind CH (eds): TNM Classification of Malignant Tumors. 6th edition. John Wiley & Sons, New York, pp65-68, 2002.
19. Lauren P: The two histological main types of gastric carcinoma: diffuse and so-called intestinal-type carcinoma. An attempt at a histo-clinical classification. Acta Pathol Microbiol Scand 64: 31-49, 1965.
20. Yasui W and Oue N: Systematic collection of tissue specimens and molecular pathological analysis of newly diagnosed solid cancers among atomic bomb survivors. Int Congr Ser: 81-86, 2007.
21. Preston DL, Pierce DA, Shimizu Y, *et al*: Effect of recent changes in atomic bomb survivor dosimetry on cancer mortality risk estimates. Radiat Res 162: 377-389, 2004.
22. Rogakou EP, Boon C, Redon C and Bonner WM: Megabase chromatin domains involved in DNA double-strand breaks *in vivo*. J Cell Biol 146: 905-916, 1999.
23. Lu C, Zhu F, Cho YY, *et al*: Cell apoptosis: requirement of H2AX in DNA ladder formation, but not for the activation of caspase-3. Mol Cell 23: 121-132, 2006.
24. Pusapati RV, Rounbehler RJ, Hong S, *et al*: ATM promotes apoptosis and suppresses tumorigenesis in response to Myc. Proc Natl Acad Sci USA 103: 1446-1451, 2006.
25. Park JH, Park EJ, Lee HS, *et al*: Mammalian SWI/SNF complexes facilitate DNA double-strand break repair by promoting gamma-H2AX induction. EMBO J 25: 3986-3997, 2006.
26. Sentani K, Oue N, Kondo H, *et al*: Increased expression but not genetic alteration of BRG1, a component of the SWI/SNF complex, is associated with the advanced stage of human gastric carcinomas. Pathobiology 69: 315-320, 2001.

RET/PTC Rearrangements Preferentially Occurred in Papillary Thyroid Cancer among Atomic Bomb Survivors Exposed to High Radiation Dose

Kiyohiro Hamatani,[1] Hidetaka Eguchi,[1,8] Reiko Ito,[1] Mayumi Mukai,[1] Keiko Takahashi,[1] Masataka Taga,[1] Kazue Imai,[1] John Cologne,[2] Midori Soda,[3] Koji Arihiro,[4] Megumu Fujihara,[5] Kuniko Abe,[9] Tomayoshi Hayashi,[9] Masahiro Nakashima,[10] Ichiro Sekine,[10] Wataru Yasui,[6] Yuzo Hayashi,[7] and Kei Nakachi[1]

Departments of [1]Radiobiology/Molecular Epidemiology, [2]Statistics, and [3]Epidemiology (Nagasaki), Radiation Effects Research Foundation, [4]Department of Pathology, Hiroshima University Hospital, [5]Department of Pathology, Hiroshima Red Cross Hospital & Atomic-bomb Survivors Hospital, [6]Department of Molecular Pathology, Hiroshima University Graduate School of Biomedical Sciences, and [7]Geriatric Health Service Facility Hidamari, Hiroshima, Japan; [8]Translational Research Center, Saitama University, International Medical Center, Saitama, Japan; and [9]Department of Pathology, Nagasaki University Hospital, and [10]Atomic Bomb Disease Institute, Nagasaki University Graduate School of Biomedical Sciences, Nagasaki, Japan

Abstract

A major early event in papillary thyroid carcinogenesis is constitutive activation of the mitogen-activated protein kinase signaling pathway caused by alterations of a single gene, typically rearrangements of the *RET* and *NTRK1* genes or point mutations in the *BRAF* and *RAS* genes. In childhood papillary thyroid cancer, regardless of history of radiation exposure, *RET/PTC* rearrangements are a major event. Conversely, in adult-onset papillary thyroid cancer among the general population, the most common molecular event is $BRAF^{V600E}$ point mutation, not *RET/PTC* rearrangements. To clarify which gene alteration, chromosome aberration, or point mutation preferentially occurs in radiation-associated adult-onset papillary thyroid cancer, we have performed molecular analyses on *RET/PTC* rearrangements and $BRAF^{V600E}$ mutation in 71 papillary thyroid cancer cases among atomic bomb survivors (including 21 cases not exposed to atomic bomb radiation), in relation to radiation dose as well as time elapsed since atomic bomb radiation exposure. *RET/PTC* rearrangements showed significantly increased frequency with increased radiation dose ($P_{trend} = 0.002$). In contrast, $BRAF^{V600E}$ mutation was less frequent in cases exposed to higher radiation dose ($P_{trend} < 0.001$). Papillary thyroid cancer subjects harboring *RET/PTC* rearrangements developed this cancer earlier than did cases with $BRAF^{V600E}$ mutation ($P = 0.03$). These findings were confirmed by multivariate logistic regression analysis. These results suggest that *RET/PTC* rearrangements play an important role in radiation-associated thyroid carcinogenesis. [Cancer Res 2008;68(17):7176–82]

Introduction

Thyroid cancer is, as is well-known, associated with exposure to external or internal ionizing radiation, such as from the atomic bombings (1) or the Chernobyl nuclear power plant accident (2, 3). The excess relative risk of thyroid cancer per Gy weighted thyroid dose was 1.15 in the Life Span Study (LSS) of atomic bomb (A-bomb) survivors (4), and a strong relationship between thyroid cancer and radiation exposure was indicated from the data of the Chernobyl accident (3). A histopathologic study has revealed that the thyroid cancers found in A-bomb survivors were largely conventional papillary in nature, and this is also the case of spontaneous thyroid cancer in the Japanese population at large. Solid variant papillary thyroid cancer (PTC) has not been found in A-bomb survivors yet, although this cancer has been frequently observed among post-Chernobyl children (5, 6).

Gene alterations that lead to constitutive activation of the mitogen-activated protein kinase (MAPK)-signaling pathway are frequently found in PTC. These alterations are mutually exclusive, nonoverlapping events that involve rearrangements of the *RET* and *neutrotrophic tyrosine kinase receptor 1* (*NTRK-1*) genes and point mutations in the *RAS* and *BRAF* genes (7–9). Alteration of one of these genes can be detected in >70% of PTC, suggesting that the constitutive activation of the MAPK-signaling pathway is a major early event in papillary thyroid carcinogenesis.

RET proto-oncogene is normally expressed in a subset of cells derived from the neural crest as well as from the kidney and the enteric nervous system (10, 11). In PTC, the *RET* proto-oncogene is activated by fusion of the *RET* TK domain with the 5′ terminal sequence of one of different heterologous genes via rearrangements that generate a series of chimeric-transforming oncogenes collectively described as *RET/PTCs*. To date, at least 12 rearranged forms of the *RET* gene have been isolated, of which *RET/PTC1* and *RET/PTC3* are by far the most common (12). *RET/PTC* rearrangements were commonly found in childhood PTC regardless of radiation history (13–15). Among the childhood PTC from areas contaminated by the Chernobyl nuclear accident in 1986, *RET/PTC3* rearrangement seemed to be strongly associated with solid variant-type PTC and with a short latency period after exposure (15, 16).

On the other hand, in the Japanese general adult population, typical frequency of *RET/PTC* seems to be of the magnitude of 10% to 40%, although a wide variation, ranging from 2.6% to 70%, has been observed in different geographic areas (17–19). *RET/PTC* rearrangements, especially *RET/PTC1*, was reported as being detected at higher frequency in PTC from adult patients with a

Note: Supplementary data for this article are available at Cancer Research Online (http://cancerres.aacrjournals.org/).

Requests for reprints: Kiyohiro Hamatani, Department of Radiobiology/Molecular Epidemiology, Radiation Effects Research Foundation, 5-2 Hijiyama Park, Minami-ku, Hiroshima-shi, Hiroshima 732-0815, Japan. Phone: 81-82-261-3169; Fax: 81-82-261-3170; E-mail: hamatani@rerf.or.jp.

doi:10.1158/0008-5472.CAN-08-0293